MASTER

Repetitive control in application with mechanical ventilators

Verkade, R.

Award date:
2019

Repetitive Control in application with Mechanical Ventilators

MASTER'S THESIS

CST 2019.050

Author:
R. Verkade
0858757

Supervisors:

ir. J.M.F. Reinders	DEMCON & TU/e
dr. ir. B.G.B. Hunnekens	DEMCON
dr. ir. T.A.E. Oomen	TU/e
prof. dr. ir. N. Van de Wouw	TU/e

Control Systems Technology
Mechanical Engineering
Eindhoven University of Technology

June 21, 2019

Technische Universiteit
Eindhoven
University of Technology

Declaration concerning the TU/e Code of Scientific Conduct for the Master's thesis

I have read the TU/e Code of Scientific Conduct[i].

I hereby declare that my Master's thesis has been carried out in accordance with the rules of the TU/e Code of Scientific Conduct

Date

21-06-2019

Name

Ruben Verkade

ID-number

0858757

Signature

Submit the signed declaration to the student administration of your department.

[i] See: https://www.tue.nl/en/our-university/about-the-university/organization/integrity/scientific-integrity/
The Netherlands Code of Conduct for Scientific Integrity, endorsed by 6 umbrella organizations, including the VSNU, can be found here also. More information about scientific integrity is published on the websites of TU/e and VSNU

Abstract

Mechanical ventilators are used for patients who cannot breathe (sufficiently) on their own. In this thesis, controller design of mechanical ventilators is considered. The control goal is to ensure good pressure tracking performance, i.e., low overshoot, rise-, and settling-time, of a pressure controlled mechanical ventilator for all possible patient types that are either fully sedated or (partly) spontaneously breathing. The main challenge in achieving this goal, is that the same mechanical ventilator is used on a wide variety of patients. Existing control strategies do not give the desired pressure tracking performance for all combinations of hoses, patients and settings. Therefore, a different approach is considered as a potential solution to improve the pressure tracking performance of mechanical ventilators.

Breathing has a repetitive nature and the target pressure of a mechanical ventilator is periodic for fully sedated patients. In this thesis, repetitive control is applied to mechanical ventilation to increase the pressure tracking performance by exploiting the repetitive nature of breathing. Repetitive control learns a disturbance model by using information from errors made in previous breaths and includes a disturbance model in the loop. Therewith, asymptotic disturbance rejection is achieved and the tracking performance in next breaths is increased.

Several repetitive controllers are designed and a comparison of their tracking performance is made. Furthermore, the best repetitive controller is compared to existing controllers in a simulation and experimental case-study. This case-study consists of fully sedated patient scenarios and spontaneously breathing patient scenarios. Due to spontaneous breathing of a patient, an unknown (possibly) aperiodic disturbance is introduced to the system. Several spontaneously breathing scenarios of interest are defined. The tracking performance of the repetitive controller compared to the existing controllers shows promising results for all the fully sedated patient- and spontaneously breathing scenarios. The main (practical) challenge for repetitive control applied to mechanical ventilation is triggered mechanical ventilation.

Acknowledgments

This thesis is a result of many things: hard work, support of all kinds, in depth discussions, relaxing, and so on. I am grateful to everyone who helped me during my graduation project, but I want to give special thanks to some people.

First of all, I want to thank my TU/e supervisors Tom Oomen and Nathan van de Wouw. Thanks for all the feedback and critical view on my graduation project. I have learned a lot from you and am very grateful for that.

Furthermore, I want to thank my DEMCON supervisors Joey Reinders and Bram Hunnekens. Thanks for all the fruitful discussions, daily supervision, and fun times. Your passion for and knowledge about mechanical ventilation have helped me enjoy this graduation project a lot. I also want to thank DEMCON, Macawi Respiratory Systems, for giving me the opportunity for this graduation project.

Last but not least, I want to thank my friends and family for supporting me all the way, even in the tough times. Very special thanks to my girlfriend, parents, brothers and parents in law for the continuous support and encouragement throughout my years of study. You helped me see the bigger picture and relax at times I needed it.

Contents

Chapter 1

Introduction

The human body relies on oxygen to stay alive. The body acquires oxygen via its respiratory system. The respiratory system ensures that the concentration levels of oxygen and carbon dioxide in the blood are adequate. In critically ill patients, the human respiratory system might fail, such that patients are unable to breathe (sufficiently) on their own. Mechanical ventilation is a treatment used to assist such patients. Mechanical ventilators are operated by a physician and commonly used in an intensive care unit (ICU) or at home for people with sleep apnea. An example of mechanical ventilation in an ICU setting is shown in Figure 1.1a.

In this project, control of mechanical ventilators is considered. Existing control methods can possibly be improved for certain patients and settings of the mechanical ventilator. Therefore, an alternative approach is pursued as a potential solution to improve the pressure support of mechanical ventilators. DEMCON, Macawi respiratory systems, develops respiratory modules, an essential part of a mechanical ventilator. An example of such a respiratory module is shown in Figure 1.1b.

In Section 1.1, the background of mechanical ventilation is described in an engineering context. Thereafter, in Section 1.2, it is described how control is applied to mechanical ventilation. Subsequently, the research goal of this thesis are given in Section 1.3. Finally, an outline of this thesis is given in Section 1.4.

1.1 Mechanical ventilation background

Often, a mechanical ventilator uses a blower to pressurize ambient air to ventilate a patient. Figure 1.2 gives a schematic overview of a mechanical ventilator, the hose, and the

(a) An example of mechanical ventilation.

(b) An example of a respiratory module.

Figure 1.1. Example of mechanical ventilation and a respiratory module, [1].

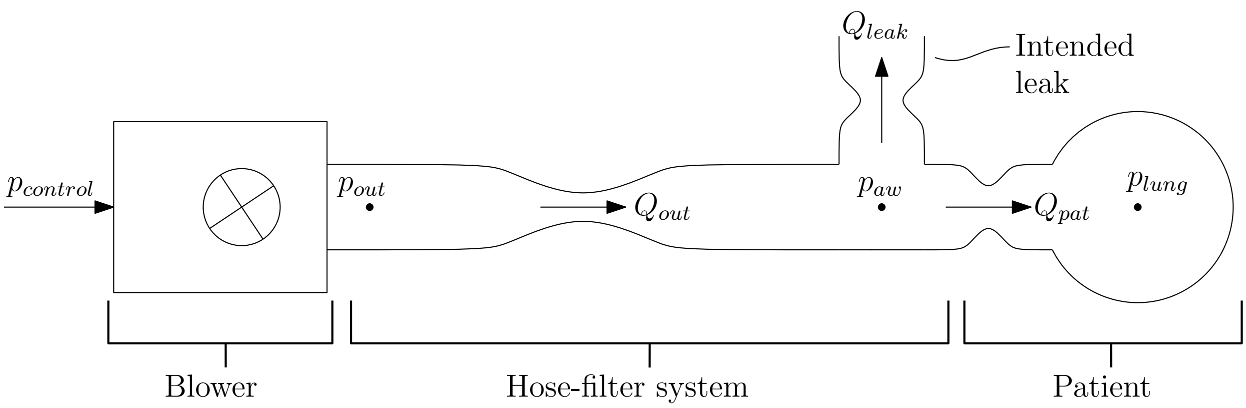

Figure 1.2. Schematic of a mechanical ventilation without a controlled expiration valve.

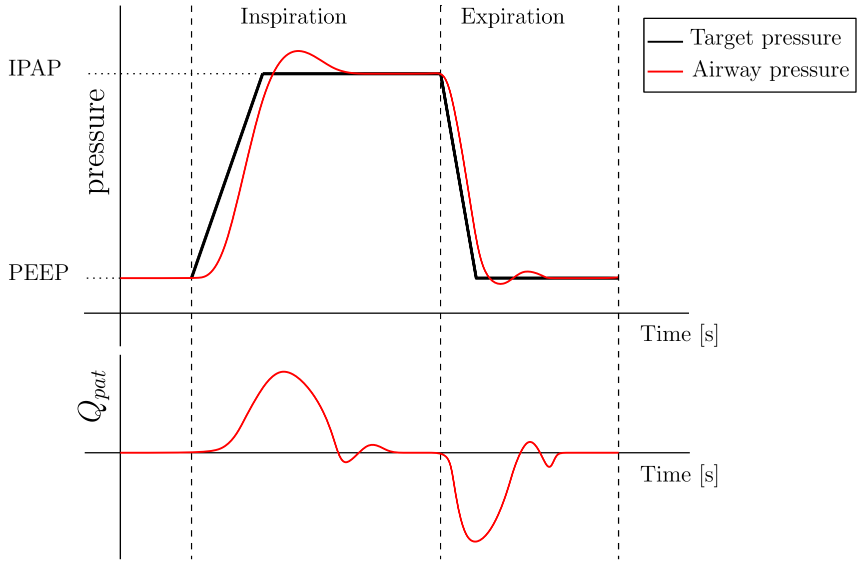

Figure 1.3. A pressure-controlled breathing cycle.

patient. In this thesis, a mechanical ventilator with passive expiration, i.e., without a controlled expiration valve, is considered. An intended leak ensures that the hose is flushed from exhaled CO_2-rich air, such that O_2-rich air is inhaled.

Pressure-controlled ventilation (PCV) is considered in this thesis, see Figure 1.3. In PCV, the minimum target pressure is the Positive End Expiratory Pressure (PEEP), which guarantees that there is always a positive pressure in the lungs, such that the alveoli (tiny air sacs in the lung that allow gas exchange) do not collapse [16]. The Inspiratory Positive Airway Pressure (IPAP) is the maximum target pressure. In PCV, the goal is to ensure that the airway pressure p_{aw} follows a time-varying pressure target p_{target}, see Figure 1.2. This change in airway pressure induces a patient flow Q_{pat}, in and out of the patient's lungs, see Figure 1.3. The desired airway pressure is achieved with a blower, i.e., the actuator. The blower has a target pressure $p_{control}$ and an outlet pressure p_{out}, see Figure 1.2. By increasing the blower outlet pressure p_{out} the pressure at the patient's airway p_{aw} is increased. The pressure difference between the blower outlet pressure p_{out} and the airway pressure p_{aw} induces an outlet flow Q_{out} through the hose. Furthermore, the intended leak near the patient's mouth induces a leak flow Q_{leak}. A target pressure profile, and resulting airway pressure and patient flow of a full breathing cycle in PCV-mode are shown in Figure 1.3.

A patient can be fully sedated or a patient can breathe spontaneously. A fully sedated patient cannot breathe on its own. Therefore, its respiration fully relies on the mechanical ventilator. When a patient breathes spontaneously, the patient might be unable to breathe sufficiently and, thus, requires some assistance from the ventilator. For spontaneously breathing patients, triggering is typically used in order to synchronize the patients breathing effort with the mechanical ventilator. The ventilator is triggered by the patient's breathing and supports it as needed. The mechanical ventilator triggers a respiration if the patient flow exceeds a physician-set threshold. Due to bad performance of the mechanical ventilator, a respiration can be falsely triggered, i.e., airway pressure overshoot caused by the controller might cause the flow threshold to be exceeded. If this occurs too often, asynchrony between the patient and ventilator may result. Such asynchrony is very uncomfortable for the patient and even associated with increased mortality rates [3].

1.2 Control applied to mechanical ventilation

Control is applied to a mechanical ventilator in order to achieve sufficient pressure support. The control goal is to ensure good pressure tracking performance of a mechanical ventilator for all possible patient types that are either fully sedated or (partly) breathe spontaneously. The main challenge in achieving this goal is that the same mechanical ventilator must deal with a wide variety of patients, hoses, and filters, i.e., large plant variations. In Section 1.2.1, the considered state-of-practice control strategies are described in detail. The state-of-practice controllers are used in practice by Macawi and are used for comparison in Chapter 4 and 5. In Section 1.2.2, state-of-the-art control strategies are presented. Thereafter, in Section 1.2.3, the envisioned solution to open issues of the considered state-of-practice and state-of-the-art control strategies is presented.

1.2.1 State-of-practice control strategies

In this section, the considered state-of-practice controls strategies are described in detail. The first considered state-of-practice controller is a **unit feedforward** (FF) controller, i.e., the feedforward signal is equal to the target pressure p_{target}, see Figure 1.4. An internal controller in the blower ensures that for frequencies up to 10 Hz, the blower target pressure $p_{control}$ and blower outlet pressure p_{out} are approximately the same, i.e., $p_{control} \approx p_{out}$. In Figure 1.6, the tracking performance of the unit feedforward controller is shown. For mechanical ventilation, the tracking performance of the unit feedforward controller might potentially be acceptable. However, the tracking performance is poor in a control engineering context. A significant steady-state tracking error Δp at the plateau pressure (from 1-1.5 seconds and 3-4 seconds) is observed. This is caused by the pressure drop over the hose.

The second considered state-of-practice controller is a **linear (integral) feedback** controller. The unit feedforward controller and the internal blower controller are used. A linear feedback controller C is added to decrease the tracking error that the feedforward controller does not compensate for, see Figure 1.4. The linear feedback controller C is tuned robustly based on FRF-measurements on mechanical test lungs to deal with large plant variations, but also to handle delays in the system. The linear (integral) feedback controller compensates for the pressure drop over the hose Δp; however, significant pressure overshoot occurs in some cases, see Figure 1.6.

The last considered state-of-practice controller is the **hose resistance compensation** controller, see Figure 1.5. The unit feedforward controller and the internal blower controller

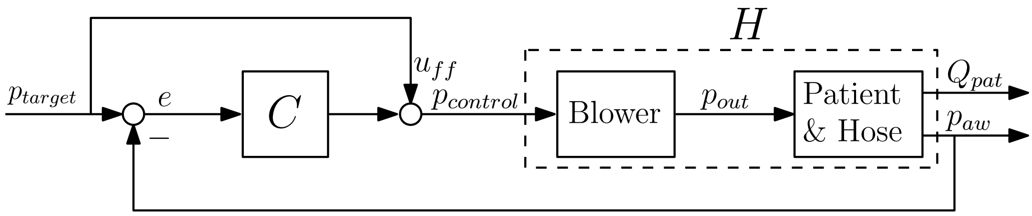

Figure 1.4. Control scheme of the unit feedforward controller, including a linear feedback controller applied to mechanical ventilation. For the unit feedforward control strategy $C = 0$ and for the linear feedback control strategy $C(s) = {}^{6.285}/_{s}$.

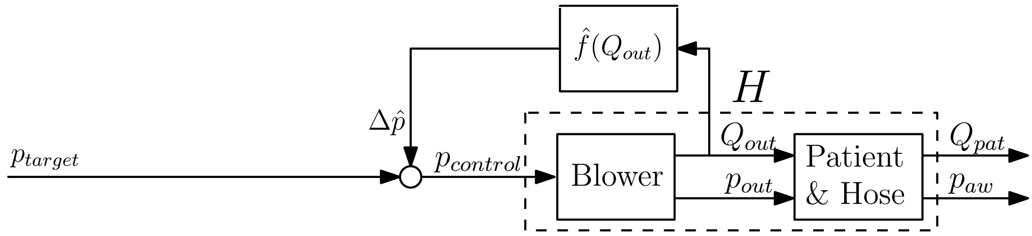

Figure 1.5. Control scheme of the hose resistance compensation controller.

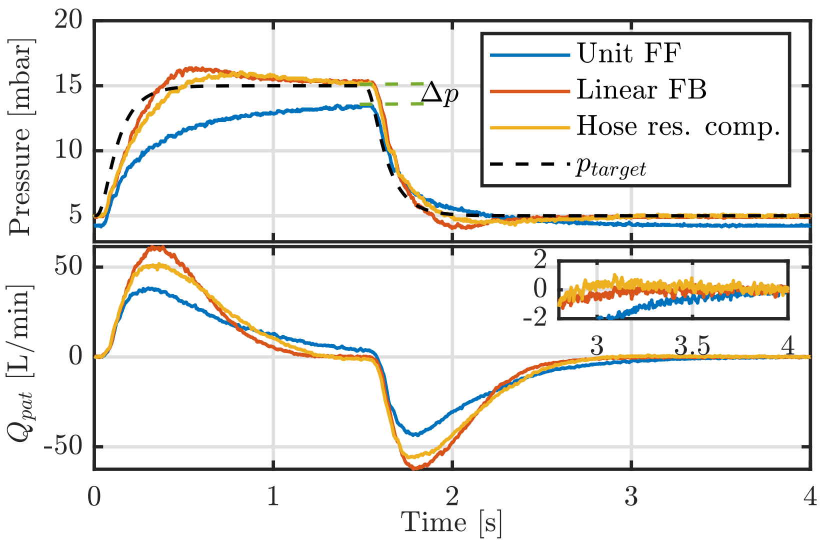

Figure 1.6. Airway pressure p_{aw} and patient flow Q_{pat} for a state-of-practice controlled breathing cycle.

are used. In addition, the pressure drop over the hose Δp is compensated for. To compensate for the pressure drop over the hose, the hose parameters should be known. The hose parameters describe the relation between the outlet flow Q_{out} and pressure drop $\Delta p = f(Q_{out})$. For this reason, an offline calibration is done to obtain an estimate of the hose parameters. Thereafter, the measurement of Q_{out} and the estimated hose parameters are used to compute an estimate of the pressure drop $\Delta\hat{p}$. In Figure 1.6, it is observed that the hose resistance compensation partly improves the tracking performance compared to the unit feedforward- and linear feedback controller. However, there is still some over overshoot in the pressure response p_{aw}, and, additionally, the pressure build-up is not sufficient. Moreover, for the hose resistance compensation, an offline calibration has to be done before it is used. This increases the workload of physicians, which is undesired.

1.2.2 State-of-the-art control strategies

Research has been done on controller design of mechanical ventilators. However, literature is limited, probably because of confidentiality of companies developing mechanical ventilators. A brief overview of the relevant publications is given here.
In [14], **variable-gain control** is applied on mechanical ventilators. This is used to balance the trade-off between fast pressure build-up and steady flow response, i.e., small flow overshoot. It is shown that a variable-gain controller outperforms the state-of-practice controllers in terms of tracking performance. However, the desired tracking performance for the wide variety of patients is not reached. In [22], an **online hose calibration** is used to estimate the hose resistance online by using measurements of p_{aw}, Q_{out}, and p_{out} in the loop. The resulting tracking performance is the same as that of the (manual) hose resistance compensation of Section 1.2.1. The main advantage of the online hose calibration is that less effort by a physician is required. Drawbacks of this method are that the blower dynamics and delays in the system are ignored. A **repetitive Model Predictive Control** (MPC) approach is used to track a periodic reference volume in a multi-compartment respiratory system in [17]. The volume tracking performance is good. However, the hose, filter, and air source are not taken into account. Besides, no experimental results, on mechanical test lungs, are shown. Therefore, it is unsure if this method works in practice. In [24], **Iterative Learning Control** (ILC) applied to mechanical ventilation is investigated. The method shows good tracking performance for a variety of patients (tested on mechanical test lungs). Shortcomings, however, are that only fully sedated patients are investigated and that the tracking performance can be even further increased. Finally, **adaptive control** is used to improve the performance of mechanical ventilators over classical PID control methods in [8]. Experiments on mechanical test lungs show a significant improvement in tracking performance for a wide variety of patients. However, the tracking performance can be further increased. The difference with [22], is that in [8] the whole plant (hose and patient) is estimated, while only the hose is estimated in [22].

1.2.3 Envisioned solution

Although the state-of-the-art control strategies all improve the tracking performance compared to the state-of-practice control strategies, the tracking performance can be increased even further. Besides, spontaneously breathing patients are not taken into account, except for the online hose calibration strategy. Improving the tracking performance is challenging, due to the following challenges:

- Patient and hose parameters are typically a priori unknown and may vary in time;
- No (unintentional) leakage information is available;
- The exact patient effort is unknown and may vary in time.

Breathing has a repetitive nature and, also, for fully sedated patients p_{target} is the same for every breath. Hence, the reference is periodic for every breath. To exploit the repetitive nature of breathing, repetitive control, [18] and [25], can potentially be used. Repetitive control adjusts the control input based on errors made in previous breaths. Repetitive control learns a disturbance model by using information from errors made in previous breaths and includes a disturbance model in the loop. Therewith, asymptotic disturbance rejection is achieved and the tracking performance in next breaths is increased. Repetitive control is a data-driven control technique and no exact model of the system is required. Therefore, it is expected that repetitive control can deal with the aforementioned challenges without requiring additional actions of a physician. In Figure 1.7, a control scheme for a repetitive controller R applied to mechanical ventilation is shown.

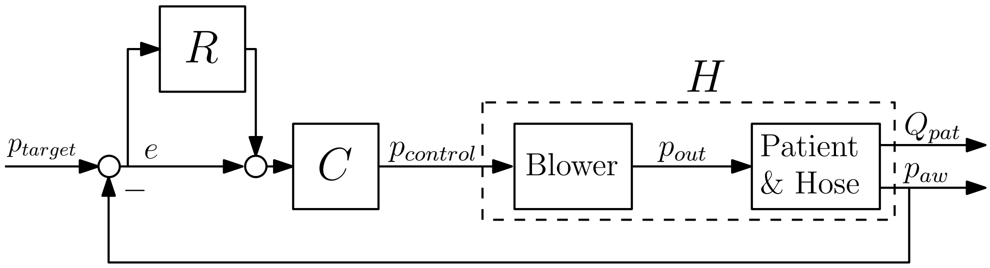

Figure 1.7. Control scheme for repetitive control applied to mechanical ventilation.

Repetitive control has been applied to a wide range of systems. In [25], repetitive control is applied to a tracking control problem of a Compact Disc player. A power supply to magnets of a synchrotron accelerator is controlled with repetitive control in [15]. Repetitive control also sees an application in industrial printers in [6]. For an extensive overview of applications, see [12].

In [24], a similar control technique as repetitive control, namely Iterative Learning Control (ILC), is applied to mechanical ventilation. As described in Section 1.2.2, the main shortcoming is that only fully sedated patients are assumed. Therefore, in this thesis, spontaneously breathing patients are also considered. Furthermore, it is expected that the tracking performance gain by using a learning control technique can be bigger.

1.3 Project goals

The goal of this project is to ensure good pressure tracking performance of a mechanical ventilator for all patient types that are either fully sedated or (partly) breathe spontaneously. As observed in Section 1.2, previous control work does not give the desired tracking performance for every combination of blower, hose, and patient. Therefore, in the scope of this project, an alternative control approach is pursued, namely repetitive control. The research goal of this thesis can be formulated as:
Investigate the potential and limitations of repetitive control applied to mechanical ventilation.

Several sub-questions are formulated and should be answered to reach this goal:

- How to design a repetitive controller that gives a good tracking performance of a mechanical ventilator for fully sedated patient scenarios?
- How does the designed repetitive controller compare to existing control strategies in:
  - fully sedated patient scenarios?
  - the presence of patient effort?
- Is it possible to apply repetitive control to triggered mechanical ventilation whilst still obtaining a good tracking performance?

1.4 Thesis outline

This thesis is structured as follows. In Chapter 2, a plant model is derived that is used for controller design and simulations. In Chapter 3, repetitive control theory is described. The essentials, stability and the design methodology of repetitive control are described. Subsequently, repetitive control is applied to a variety of fully sedated patient scenarios in Chapter 4. Both simulations and experiments are conducted to compare the tracking performance of repetitive control with the state-of-practice controllers. In Chapter 5, the challenge in applying repetitive control to spontaneously breathing patients is described. Thereafter, a comparison of the tracking performance of repetitive control and the state-of-practice controllers applied to mechanical ventilation of spontaneously breathing patients is given. Finally, in Chapter 6, conclusions are drawn and the research goal of Section 1.3 is reflected upon. Also, recommendations for future work are given.

Chapter 2

System Modeling

In this chapter, a plant model is derived. This plant model is used for simulations and controller design in Chapter 4 and 5. In Section 2.1, the plant model is derived. The plant consists of a patient, hose-filter, and a blower-driven mechanical ventilator. Finally, this chapter is summarized in Section 2.2.

2.1 Patient-hose-blower model

This section describes the plant model, consisting of a patient-, hose-filter-, and a blower model. The plant model is divided into multiple subsystems, which are derived using first-principle modeling. First, the patient model is given, consisting of the lungs and airway, see Section 2.1.1. Thereafter, the hose-filter model is derived and combined with the patient model, see Section 2.1.2. Subsequently, the blower model is given, see Section 2.1.3. Finally, in Section 2.1.4, the patient-hose model is combined with the blower model. This results in the plant model without delays.

2.1.1 Patient model

The patient is modeled by combining a lung compliance model with an airway resistance model. Both are modeled separately and, thereafter, the lung- and airway model are combined, resulting in the patient model. A linear single-compartment model is used for the patient model, see [2, Chapter 3].

Lung Model

A schematic of the lung is shown in Figure 2.1.
The lung model has a compliance, C_{lung}, an internal pressure, p_{lung}, and the patient flow, Q_{pat}, is going in and out of the lungs. Compliance is inverse-stiffness, hence, a compliant lung is a non-stiff lung and vice-versa. C_{lung} gives the following relation between the lung volume V_{pat} and the lung pressure p_{lung}:

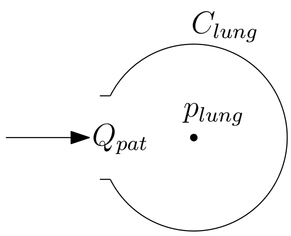

Figure 2.1. Schematic of the lung.

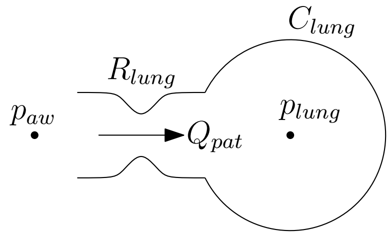

Figure 2.2. Schematic of the patient, consisting of the lung and airway.

$$C_{lung} = \frac{V_{pat}(t)}{p_{lung}(t)}. \tag{2.1}$$

Substituting $V_{pat}(t) = \int Q_{pat}(t)dt$ in (2.1) and rewriting gives:

$$p_{lung}(t) = \frac{\int Q_{pat}(t)dt}{C_{lung}}. \tag{2.2}$$

Taking the derivative with respect to time of (2.2), leads to the linear differential equation for the lungs:

$$\dot{p}_{lung}(t) = \frac{Q_{pat}(t)}{C_{lung}}. \tag{2.3}$$

Patient airway model

The patient's airway connects the mouth to the lungs and is modeled as a linear resistance. A schematic representation of the airway and lungs is depicted in Figure 2.2. Since Q_{pat} in ventilation is typically small, it is valid to assume a linear airway resistance R_{lung}. In this figure, R_{lung} is the resistance of the airway and Q_{pat} is defined as:

$$Q_{pat}(t) = \frac{p_{aw}(t) - p_{lung}(t)}{R_{lung}}. \tag{2.4}$$

By substituting (2.4) in (2.3), the following differential equation for the lung pressure is obtained:

$$\dot{p}_{lung}(t) = \frac{p_{aw}(t) - p_{lung}(t)}{C_{lung}R_{lung}}. \tag{2.5}$$

2.1.2 Patient-hose model

During mechanical ventilation, the patient is connected to a hose-filter system. Together this forms the patient-hose system, shown in Figure 2.3. Note that ambient pressure is considered to be zero, since all pressures are defined with respect to the ambient pressure. In the hose, a pressure drop $\Delta p = p_{out} - p_{aw}$ occurs. In Figure 2.4, a measurement of the pressure drop Δp for positive outlet flows Q_{out} is shown. Three least-squares fits are made on the measurement data, a quadratic and two linear fits. The quadratic fit is of the form

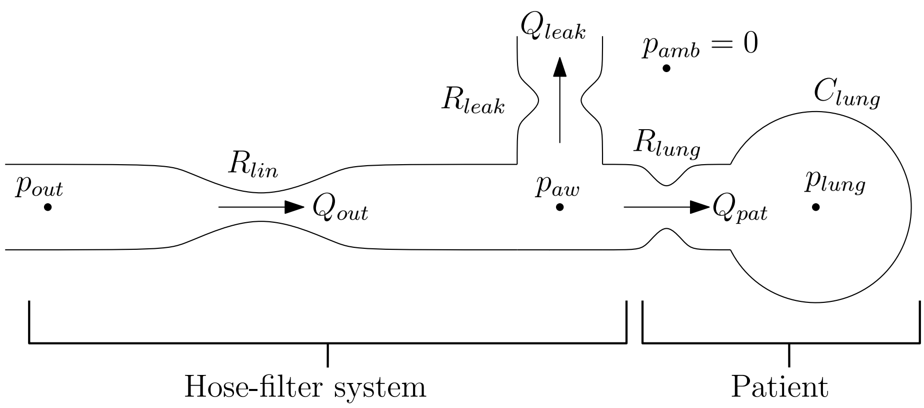

Figure 2.3. Schematic of patient-hose system

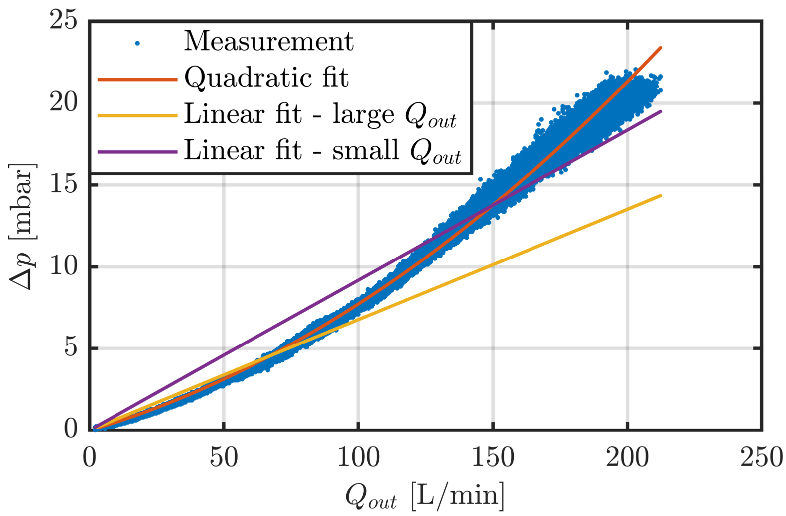

Figure 2.4. A measurement and several fits of the pressure drop over the hose Δp over the outlet flow Q_{out}.

$$\Delta p = R_{lin} Q_{out} + R_{quad} Q_{out} |Q_{out}|. \tag{2.6}$$

It is observed that the quadratic fit matches the measurement accurately. The linear fits are of the form

$$\Delta p = R_{lin} Q_{out}. \tag{2.7}$$

The first linear fit is made for small flows, namely $Q_{out} < 100$L/min, and the other linear fit for large flows, namely $Q_{out} < 250$L/min. It is observed that the linear fit for large flows does not match the measurement accurately, however, the linear fit for small flows matches the measurements significantly better for small flows. The hose-resistance R_{lin} is modeled linear for control purposes.
The hose contains an intended leak near the patient to flush the system from exhaled, CO_2-rich, air such that O_2-rich air is inhaled. The intended leak is also modeled as a linear resistance R_{leak}.

The hose-filter system and the patient are combined, by using conservation of flow, i.e., the incoming flow is equal to the outgoing flow. This gives the following relation between the flows in the system:

$$Q_{pat}(t) = Q_{out}(t) - Q_{leak}(t). \tag{2.8}$$

Where the patient flow $Q_{pat}(t)$ is defined in (2.4). Furthermore, the outlet flow $Q_{out}(t)$ and the leak flow $Q_{leak}(t)$ are defined as:

$$Q_{out}(t) = \frac{p_{out}(t) - p_{aw}(t)}{R_{lin}}, \tag{2.9}$$

$$Q_{leak}(t) = \frac{p_{aw}(t)}{R_{leak}}. \tag{2.10}$$

By substituting (2.4), (2.9), and (2.10) in (2.8), it follows that:

$$\frac{p_{aw}(t) - p_{lung}(t)}{R_{lung}} = \frac{p_{out}(t) - p_{aw}(t)}{R_{lin}} - \frac{p_{aw}(t)}{R_{leak}}. \tag{2.11}$$

Rewriting (2.11), gives

$$p_{aw}(t) = \frac{R_{lin}R_{leak}}{\bar{R}} p_{lung}(t) + \frac{R_{leak}R_{lung}}{\bar{R}} p_{out}(t) \tag{2.12}$$

with $\bar{R} = R_{leak}R_{lin} + R_{leak}R_{lung} + R_{lin}R_{lung}$.
By substituting (2.12) in (2.5), the patient-hose model is obtained

$$\dot{p}_{lung}(t) = -\frac{R_{leak} + R_{lin}}{\bar{R}C_{lung}} p_{lung}(t) + \frac{R_{leak}}{\bar{R}C_{lung}} p_{out}(t). \tag{2.13}$$

This differential equation describes the rate of change of the lung pressure, $\dot{p}_{lung}(t)$, as a function of the state $p_{lung}(t)$ and input $p_{out}(t)$.

The considered measured output variables are $Q_{pat}(t)$ and $p_{aw}(t)$. The output expression for p_{aw} is given in (2.12). The expression for $Q_{pat}(t)$ is found by substituting (2.12) in (2.4), resulting in

$$Q_{pat}(t) = -\frac{R_{leak} + R_{lin}}{\bar{R}} p_{lung}(t) + \frac{R_{leak}}{\bar{R}} p_{out}(t). \tag{2.14}$$

State-space formulation

Here, the patient-hose model is written in state-space formulation. The patient-hose state x_{ph}, input u_{ph}, and outputs y_{ph} are defined as:

$$x_{ph} := p_{lung}, \quad u_{ph} := p_{out}, \text{ and } \quad y_{ph} := \begin{bmatrix} p_{aw} & Q_{pat} \end{bmatrix}^T, \tag{2.15}$$

respectively. This results in the state-space system:

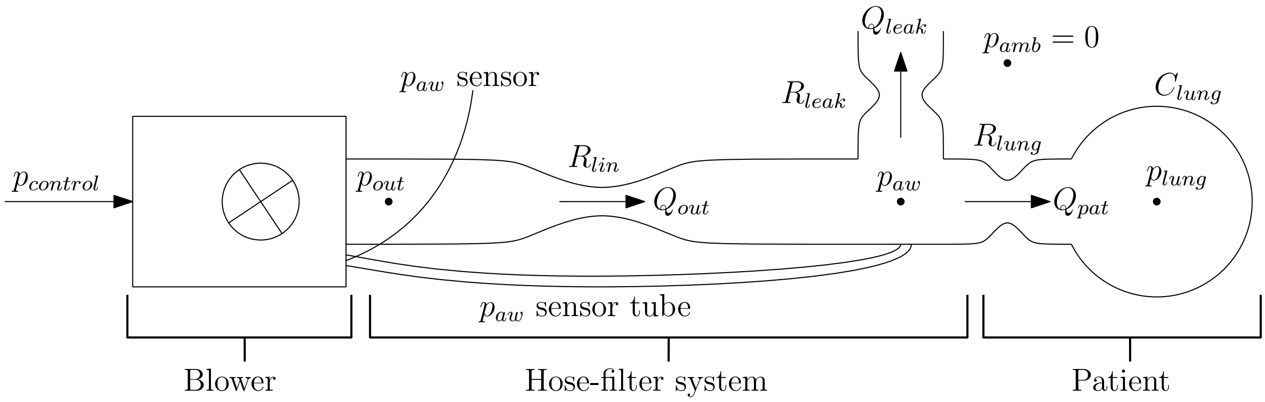

Figure 2.5. Schematic of patient-hose system with blower.

$$\begin{aligned} \dot{x}_{ph} &= \underbrace{-\frac{R_{leak}+R_{lin}}{\bar{R}C_{lung}}}_{A_{ph}} x_{ph} + \underbrace{\frac{R_{leak}}{\bar{R}C_{lung}}}_{B_{ph}} u_{ph}, \\ y_{ph} &= \underbrace{\begin{bmatrix} \frac{R_{lin}R_{leak}}{\bar{R}} & -\frac{R_{leak}+R_{lin}}{\bar{R}} \end{bmatrix}^T}_{C_{ph}} x_{ph} + \underbrace{\begin{bmatrix} \frac{R_{leak}R_{lung}}{\bar{R}} & \frac{R_{leak}}{\bar{R}} \end{bmatrix}^T}_{D_{ph}} u_{ph}. \end{aligned} \tag{2.16}$$

It is seen that $A_{ph} = -\frac{R_{leak}+R_{lin}}{\bar{R}C_{lung}} < 0$, since $\{R_{lung}, C_{lung}, R_{lin}, R_{leak}\} \in \mathbb{R}_{>0}$. Therefore, the obtained patient-hose system is asymptotically stable.

2.1.3 Blower model

The final part of the plant is the blower-driven mechanical ventilator, or simply a blower. In Figure 2.5, it is seen that the plant consists of the blower and the patient-hose model. The blower is an actuator with set-point $p_{control}$ that creates an output pressure p_{out} and, therewith, an outlet flow Q_{out}.

An internal controller is present in the blower. This internal controller ensures that for frequencies up to 10 Hz, the blower target pressure $p_{control}$ is approximately the same as the blower outlet pressure p_{out}, i.e., $p_{control} \approx p_{out}$. The blower, including internal controller, is modeled as a second-order low-pass filter

$$B(s) = \frac{p_{out}(s)}{p_{control}(s)} = \frac{\omega_n^2}{s^2 + 2\zeta\omega_n s + \omega_n^2}, \tag{2.17}$$

where $B(s)$ is the transfer-function of the blower-model, $\zeta = 1$ and $\omega_n = 2\pi 30$ rad/s. To combine the blower with the patient-hose model, (2.17) is rewritten into state-space form. The blower states x_b, input u_b, and output y_b are, defined as

$$x_b \in \mathbb{R}^2, \quad u_b := p_{control}, \text{and} \quad y_b := p_{out}, \tag{2.18}$$

respectively. This results in the following state-space system:

$$\begin{aligned} \dot{x}_b &= \underbrace{\begin{bmatrix} -2\omega_n & -\omega_n^2 \\ 1 & 0 \end{bmatrix}}_{A_b} x_b + \underbrace{\begin{bmatrix} 1 & 0 \end{bmatrix}^T}_{B_b} u_b, \\ y_b &= \underbrace{\begin{bmatrix} 0 & \omega_n^2 \end{bmatrix}}_{C_b} x_b. \end{aligned} \tag{2.19}$$

It is seen that $\lambda_{1,2_{A_b}} = -\omega_n < 0$, since $\omega_n \in \mathbb{R}_{>0}$, where $\lambda_{1,2_{A_b}}$ are the eigenvalues of A_b. Thus, the blower described by (2.17) is asymptotically stable.

2.1.4 Combining the patient-hose model with the blower

Here, the patient-hose model (2.16) is combined with the blower model (2.19). Note that the output of the blower model is equal to the input of the patient-hose model. Therefore, the plant model is derived by computing the cascade of the patient-hose model and blower model. The states x, input u, and outputs y, of the plant model are defined as

$$x := \begin{bmatrix} x_b \\ x_{ph} \end{bmatrix}, \quad u := p_{control}, \text{and} \quad y := \begin{bmatrix} p_{aw} & Q_{pat} \end{bmatrix}^T, \tag{2.20}$$

respectively. This results in the following state space formulation:

$$\begin{aligned} \dot{x} = \begin{bmatrix} \dot{x}_b \\ \dot{x}_{ph} \end{bmatrix} &= \underbrace{\begin{bmatrix} A_b & 0 \\ B_{ph}C_b & A_{ph} \end{bmatrix}}_{A} \begin{bmatrix} x_b \\ x_{ph} \end{bmatrix} + \underbrace{\begin{bmatrix} B_b \\ 0 \end{bmatrix}}_{B} u, \\ y = \begin{bmatrix} p_{aw} & Q_{pat} \end{bmatrix} &= \underbrace{\begin{bmatrix} D_{ph}C_b & C_{ph} \end{bmatrix}}_{C} \begin{bmatrix} x_b \\ x_{ph} \end{bmatrix}. \end{aligned} \tag{2.21}$$

Since the patient-hose-blower system, i.e., the plant, is defined as a cascade connection of two asymptotically stable LTI systems, the plant is asymptotically stable.

2.2 Summary

In this chapter, the plant model has been derived. The plant model consists of several submodels, namely a patient model, hose-filter model and a blower model. After deriving models for each part of the plant, the models have been combined, obtaining the plant model.

Chapter 3

Repetitive Control Theory

In this chapter, repetitive control theory is described in detail. In Section 3.1, a brief comparison of Iterative Learning Control (ILC) and repetitive control is given. Then, in Section 3.2, the basic principles of repetitive control are presented. Thereafter, in Section 3.3, the stability of repetitive control is analyzed. Subsequently, in Section 3.4, the design methodology of repetitive control is treated. Finally, this chapter is summarized in Section 3.5.

3.1 Iterative learning control and repetitive control

In this section, a brief comparison of ILC, [26] and [20], and repetitive control, [18] and [25], is given. Both ILC and repetitive control are typically used in dynamical systems that operate repetitively, [19]. By learning from errors made in previous tasks, the tracking performance can be improved. In Figure 3.1a and 3.1b, a typical disturbance is given that can be attenuated by ILC and repetitive control, respectively. An essential difference between ILC and repetitive control are the requirements on the initial conditions. For ILC, the initial conditions are equal for every trial $x(0) = x(N) = x(2N) = x_0$ with $x_0 \in \mathbb{R}$ and N the trial length in samples. Iterative learning control resets the initial condition after every trial and operates over independent iterations. Therefore, ILC consists of a time- and trial-domain, i.e., it is a 2-D control structure. For repetitive control, the initial conditions $x(0) = x_0$, however, $x(N)$, $x(2N)$, and $x(3N)$ depend on previous inputs since repetitive control does not reset after operation has started. Therewith, repetitive controller is a 1-D feedback controller. Hence, classical feedback theory, e.g., Nyquist's stability criterion, applies to repetitive control. Since breathing does not reset after every breath, repetitive control is used instead of ILC in this thesis.

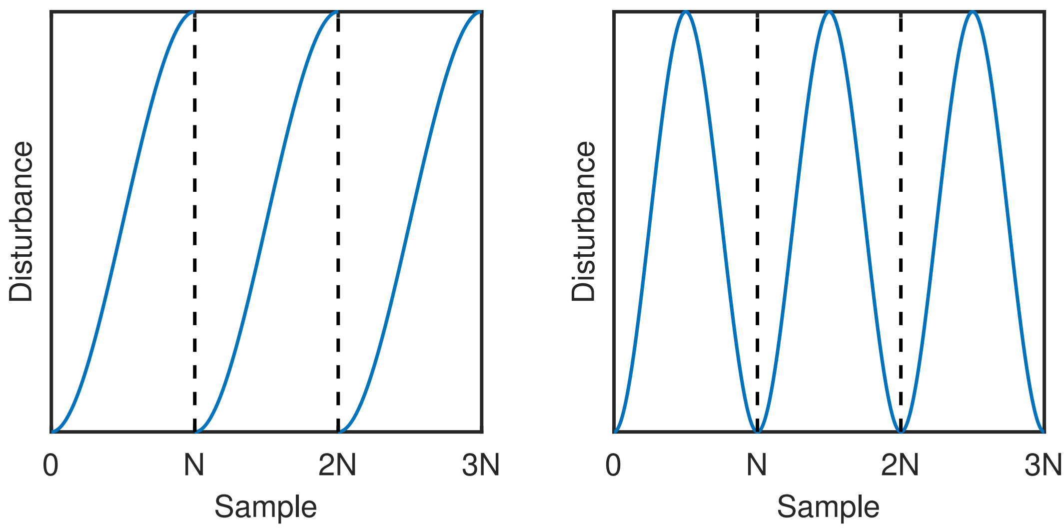

(a) Repeating disturbance that can be attenuated by ILC.

(b) Periodic disturbance that can be attenuated by repetitive control.

Figure 3.1. Typical disturbances that can be attenuated by ILC and repetitive control, [4].

3.2 Basic principles of repetitive control

This section describes the basics of repetitive control. In Section 3.2.1, the Internal Model Principle (IMP) is introduced, including illustrative examples to show the working principle of the IMP. Thereafter, in Section 3.2.2, it is shown how to add repetitive control to an existing control scheme.

3.2.1 Internal Model Principle

The basic idea of repetitive control was first shown in [15]. The fundamentals on stability and controller design are shown in [11] and [28]. In essence, repetitive control is based on the Internal Model Principle (IMP) [9]. The IMP states that *asymptotic disturbance rejection is achieved if a model of the disturbance generating system is included in a stable feedback loop*. Next, two illustrative examples are given to show the working principle of the IMP [4]. These examples are given in discrete-time, since the repetitive controllers in this thesis are also designed in discrete-time.

Step disturbance

As an example of the IMP, consider a step disturbance:

$$d(k) = \begin{cases} 1, \text{for } k \geq 0 \\ 0, \text{for } k < 0 \end{cases} . \tag{3.1}$$

By taking the $z-$transform of $d(k)$, one finds that:

$$D(z) = \frac{1}{1 - z^{-1}}, \tag{3.2}$$

where z is the discrete Laplace-variable.
In Figure 3.2 the model of a step-disturbance $d(k)$ (3.2) is depicted in a block scheme. A step-disturbance is given as input for one sample and, thereafter, the input is zero. It is

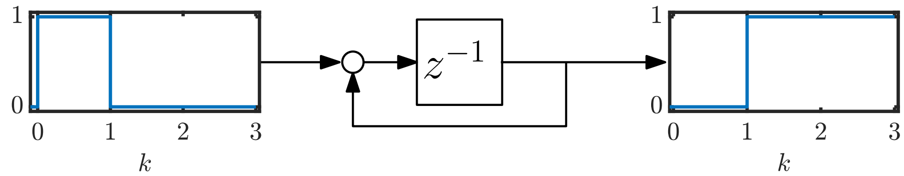

Figure 3.2. Disturbance generating system for a step disturbance.

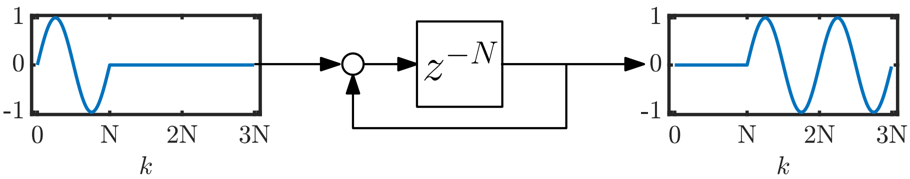

Figure 3.3. Disturbance generating system for an arbitrary periodic disturbance with period N.

observed that the disturbance generating system, i.e., the discrete integrator, generates the step-disturbance even after the input is zero. Furthermore, it is observed that the disturbance is a periodic signal with period one.

Arbitrary periodic disturbance

Now consider an arbitrary periodic disturbance with period N. In that case the disturbance generating system, or disturbance model, is a series of integrators. This is visualized in Figure 3.3. One period of a periodic disturbance with period N is put into a series of integrators and, thereafter, the input is zero. It is observed that the series of integrators generate the periodic disturbance with period N, even after the input is zero.

3.2.2 Repetitive control in an existing control scheme

This section describes how to include repetitive control in an existing control scheme. Note that this is done in discrete-time throughout this thesis. In previous section it has been shown that a series of integrators generates a periodic disturbance. If one adds the series of integrators to an existing (asymptotically stable) control loop, as shown in Figure 3.4, the series of integrators are an error-driven disturbance model. Therewith, asymptotic rejection of periodic disturbances, e.g., a periodic reference r or periodic disturbances d, is achieved. The repetitive controller R amplifies the error e at harmonic frequencies, in which the fundamental frequency matches the inverse of the period of the periodic disturbance, see Figure 3.5a. In terms of disturbance rejection, the repetitive controller modifies the transfer from r to e, i.e., the sensitivity, see Figure 3.5b. It is observed that, compared to the sensitivity without repetitive control, r is rejected at the harmonic frequencies of the period of r. Therewith, asymptotic rejection of periodic disturbances is achieved. Note that the control scheme needs to be (asymptotically) stable in order to asymptotically reject the periodic disturbances. In Section 3.3, concrete mathematical expressions of the repetitive controller R and the sensitivity are given, including a stability analysis of the closed-loop controlled system.

3.3 Stability

In this section, stability conditions of repetitive control are presented, resulting in a necessary and sufficient-, and a sufficient stability condition, see [18]. In Figure 3.6, the same

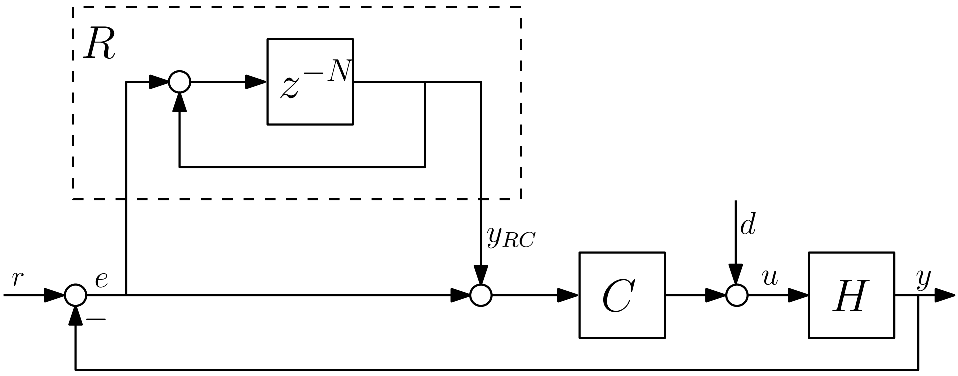

Figure 3.4. Repetitive control added on to a typical control scheme.

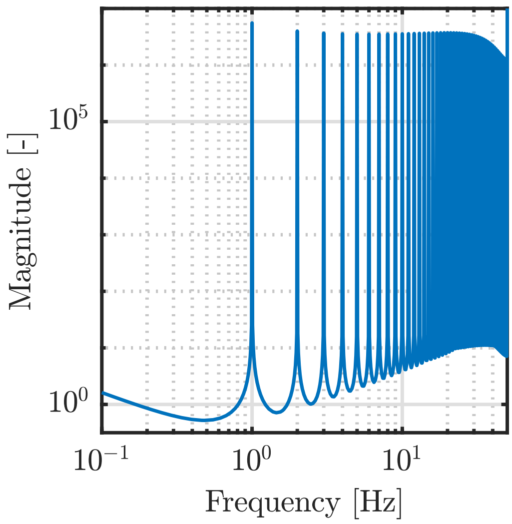

(a) Magnitude of the repetitive controller R.

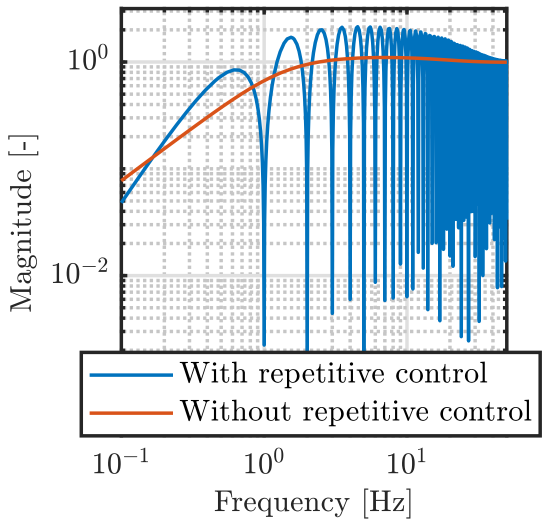

(b) Sensitivity function for add-on repetitive control.

Figure 3.5. Essential transfer functions for a repetitive controller with period of r equal to 1 s.

control scheme as Figure 3.4 is shown, however, a learning filter L and robustness filter Q are added to the repetitive controller. In Section 3.4, L and Q are explained in more detail. In Figure 3.6, r is a periodic reference with period N, C is a feedback controller, H is the plant, R is the repetitive controller, d is an input-disturbance, y_{RC} is the output of the repetitive controller, y is the output, and e is the tracking error.
The transfer function from the tracking error e to the output of the repetitive controller $y_{RC} = Re$ is

$$R = \frac{z^{-N}LQ}{1 - z^{-N}Q}. \tag{3.3}$$

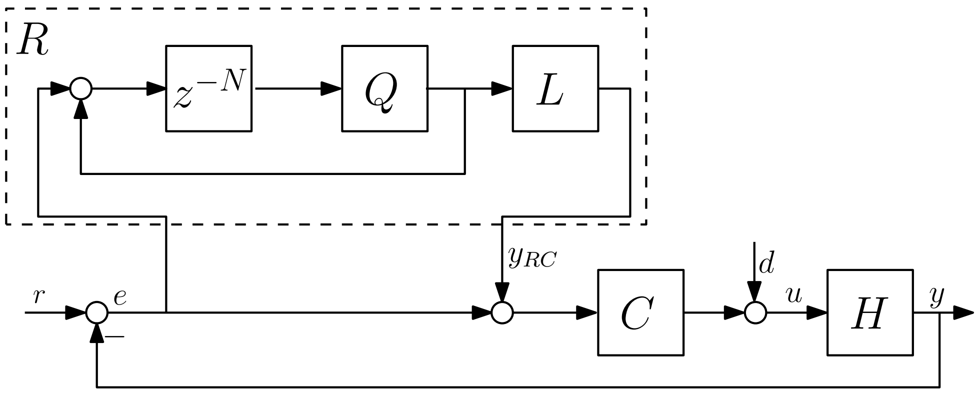

Figure 3.6. Closed-loop system with add-on repetitive control, including learning filter L and robustness filter Q.

An expression for the tracking error $e = r - y$ is derived as follows:

$$
\begin{aligned}
e &= (1 + HC(1 + R))^{-1}(r - Hd) && (3.4)\\
&= (1 + HC + (1 + HC)(1 + HC)^{-1}HCR)^{-1}(r - Hd) && (3.5)\\
&= \underbrace{(1 + TR)^{-1}}_{S_R}\underbrace{(1 + HC)^{-1}}_{S}(r - Hd) && (3.6)\\
&= S_R S(r - Hd), && (3.7)
\end{aligned}
$$

where S_R is called the modifying sensitivity and $T = (1 + HC)^{-1}HC = 1 - S$ the complimentary sensitivity with $R = 0$. It is assumed that the sensitivity S, the process-sensitivity SH and the complementary sensitivity T are asymptotically stable due to design of C. Using this assumption and (3.7), it follows that the closed-loop is asymptotically stable if S_R is asymptotically stable.

By substituting (3.3) in S_R, from (3.6), and rewriting, it is obtained that

$$S_R = \frac{1 - z^{-N}Q}{1 - z^{-N}Q(1 - TL)}. \tag{3.8}$$

From (3.8), a necessary and sufficient stability condition for repetitive control is derived, see Theorem 1 (see [18] Theorem 1 and 2 and [5]).

Theorem 1 (Necessary and sufficient stability condition for repetitive control) *Assume S and T are asymptotically stable. Then, S_R is asymptotically stable if and only if the Nyquist plot of $-z^{-N}Q(1 - TL)$*

- *makes no encirclements of the point -1, and*
- *does not pass through the point -1.*

It is complex to see whether $-z^{-N}Q(1 - TL)$ makes encirclements of the -1 point, due to the following reasons:

- In most physical systems $|S| > 1$ for some frequencies, due to the Bode sensitivity integral.
- z^{-N} gives a 360° phase-shift every $1/NT_s$ Hz, with T_s the sample-time.

Therefore, a sufficient condition for stability, based on the small-gain theorem, is used in practice, see Theorem 2.

Theorem 2 (Sufficient stability condition for repetitive control) *Assume S and T are asymptotically stable. Then, S_R is asymptotically stable for all N if*

$$|Q(1 - TL)| < 1, \forall z = e^{i\omega}, \omega \in [0, 2\pi),$$

which is a special case of the multivariable case, see [18] Theorem 4. Essentially, this means that $-z^{-N}Q(1 - TL)$ stays inside the unit-circle and, therewith, encirclements of the -1 point never occur. An important difference between Theorem 1 and 2 is that Theorem 2 holds for all values of N. Therewith, design based on Theorem 2 is independent of N. For a fixed T, one should shape L and Q such that stability is ensured. In the next section, design of L and Q is treated in more detail.

3.4 Filter design

This section describes the design methodology of the learning- and robustness-filter, L and Q, respectively. In Section 3.4.1, design of the learning filter L is explained. Thereafter, in Section 3.4.2, design of the robustness filter Q is explained. Illustrative examples are given to show how L and Q affect stability and performance. Finally, in Section 3.4.3, a typical design procedure for a repetitive controller is presented.

3.4.1 Learning filter design

In this section, design of the learning filter L is described in detail. From Theorem 2, it is seen that if $L = T^{-1}$ and $Q = 1$, then $|Q(1 - TL)| = 0$. Hence, the closed-loop, containing a repetitive controller, is asymptotically stable for every N. One cannot always simply invert T to obtain L, however, due to the following reasons:

- If T is strictly proper, T^{-1} is improper and, therewith, non-causal. Non-causal filtering requires knowledge of future outputs, which is unavailable;
- If T is non-minimum phase, T^{-1} is unstable. Including an unstable L to an existing stable closed-loop, results in an unstable closed-loop.

To overcome these problems, several techniques have been developed in literature, such as Zero Phase Error Tracking Control (ZPETC), [27], Non-minimum Phase Zeros Ignore (NPZ-Ignore), [10], Extended Bandwidth Zero Phase Error Tracking Control (EBZPETC), [29], and stable-inversion, [30]. In this thesis, ZPETC is used to compute an asymptotically stable and non-causal inverse of the complementary sensitivity T. Note that ZPETC requires a (parametric) model to compute the non-causal inverse.

For a strictly proper T, T^{-1} is improper and, hence, non-causal. Non-causal filtering requires knowledge of future outputs, which is unavailable. Therefore, ZPETC computes a causal learning filter L_c. This causal L_c is used to obtain a non-causal learning filter

$$L = z^{p+d} L_c, \tag{3.9}$$

where p is the relative degree of T and d is the number of samples delays in T. This non-causal learning filter L can be implemented, since the repetitive controller contains a delay of N samples, see Figure 3.6. Therefore, implementing the non-causal L is possible for $p + d \leq N$, since N can be replaced by $N - (p + d)$. By computing L with (3.9), the phase of TL is zero, i.e., zero-phase error between T and L, as depicted in both Bode plots of Figure 3.7.

For a non-minimum phase T, i.e., T contains zeros outside the unit circle, T^{-1} is unstable. To avoid instability of the inverse, ZPETC ignores the zeros outside the unit circle. Therewith, an approximate inverse of T is computed. In Figure 3.8, the error 2-norm $||e||_2$, or

Euclidean norm, is shown for a minimum- and non-minimum phase system. The error 2-norm $||e||_2$ is defined as:

$$||e||_2 = \sqrt{\sum_i |e_i|^2}, \tag{3.10}$$

where i is the sample in a breath. In Figure 3.7a it is observed that the minimum phase system yields an exact inverse of T. Hence, $TL = 1$ and, thus, (3.8), is zero for the harmonics of the periodic disturbance. Therefore, the error 2-norm in Figure 3.8 converges in 1 breath. For the non-minimum phase system, an approximate inverse is computed, see Figure 3.7b. Hence, $TL \approx 1$ and, thus (3.8), is approximately zero for the harmonics of the periodic disturbance. Therefore, the convergence rate of the error 2-norm in Figure 3.8 is lower compared to the minimum phase system.

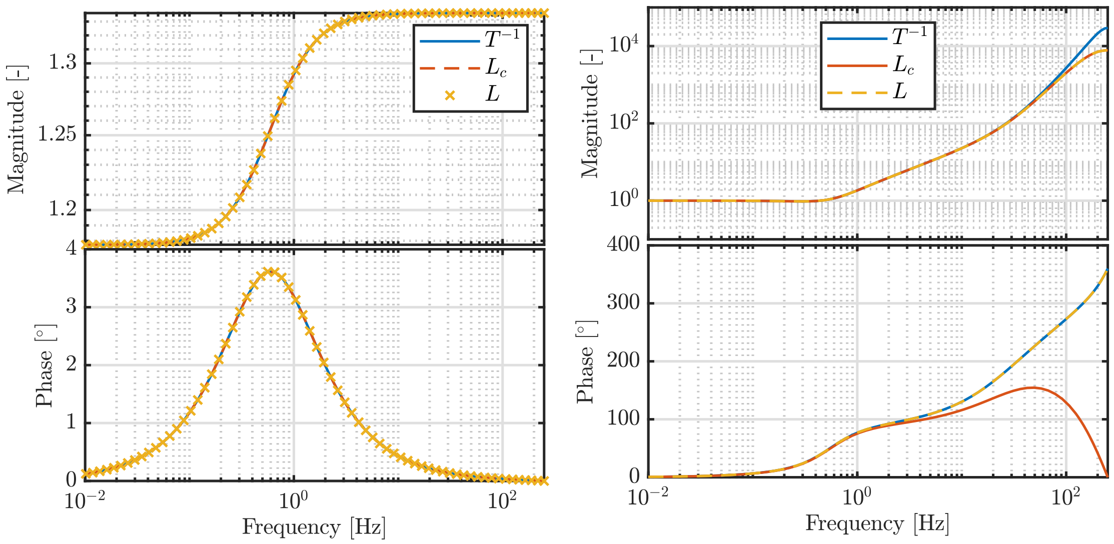

(a) For a minimum phase system, where $C = 1$ and H is the zero-order hold discretized patient-hose system (2.16).

(b) For a non-minimum phase system, where $C(z) = 6.285 \frac{T_s}{2} \frac{z+1}{z-1}$ and H is the zero-order hold discretized patient-hose-blower system (2.21).

Figure 3.7. Bode plots of the inverse of $T = {CH}/{1+CH}$, and the causal- and non-causal L-filter.

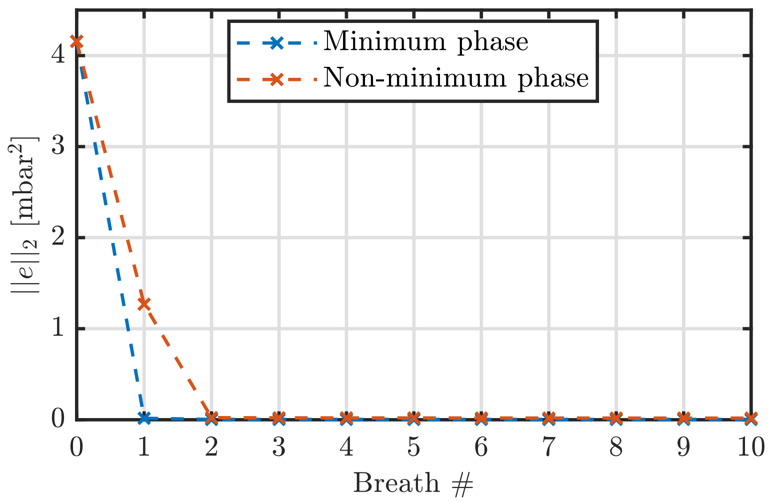

Figure 3.8. Error 2-norm of 10 breaths of the same minimum phase and non-minimum phase system as Figure 3.7.

Handling aperiodic disturbances using a learning gain

Throughout this section, only periodic disturbances are considered. However, typically, aperiodic disturbances are also present in a system. These disturbances are not periodic with the buffer length N, such as noise. Aperiodic disturbances can contain all frequencies and not necessarily harmonic frequencies of the periodic disturbance. In Figure 3.5b, it is observed that for frequencies other than the harmonic frequencies of the periodic disturbance, the sensitivity is often higher than 1. Therefore, aperiodic disturbances are not rejected, but amplified by the repetitive controller. Therewith, the attenuation of the aperiodic disturbances relies only on the linear feedback controller C. Since, C is tuned for robustness, the tracking error e after convergence is non-zero in the presence of aperiodic disturbances.
A method to deal with amplification of aperiodic disturbances, is by using a learning gain α, as follows

$$L_\alpha = \alpha L, \tag{3.11}$$

where $\alpha \in [0, 1]$. For $\alpha = 0$ $R = 0$, thus, no learning occurs and for $\alpha = 1$ L is equivalent to L_α. Next, an example is used to show the influence of the learning gain.
In Figure 3.9a, it is observed that the sensitivity for the case where $\alpha = 0.5$ is lower for most frequencies compared to the case where $\alpha = 1$. Note that $\alpha = 1$ corresponds to the case where $L = L_\alpha$. The effect of the lower sensitivity is two fold:

- The sensitivity is lower for every harmonic of the periodic disturbance. Therewith, the learning filter with learning gain L_α is not equal to an exact inverse of the complimentary sensitivity of the true system, therefore, the convergence rate decreases, see Figure 3.9b. The reduction in convergence rate is explained in the comparison of the minimum- and non-minimum phase systems, see Figure 3.8.
- The sensitivity is also lower for most other frequencies than the harmonics of the periodic disturbance. Therewith, amplification of aperiodic disturbances is reduced. Therefore, a lower error 2-norm is obtained upon convergence, see Figure 3.9b.

Throughout the rest of this thesis $\alpha = 1$.

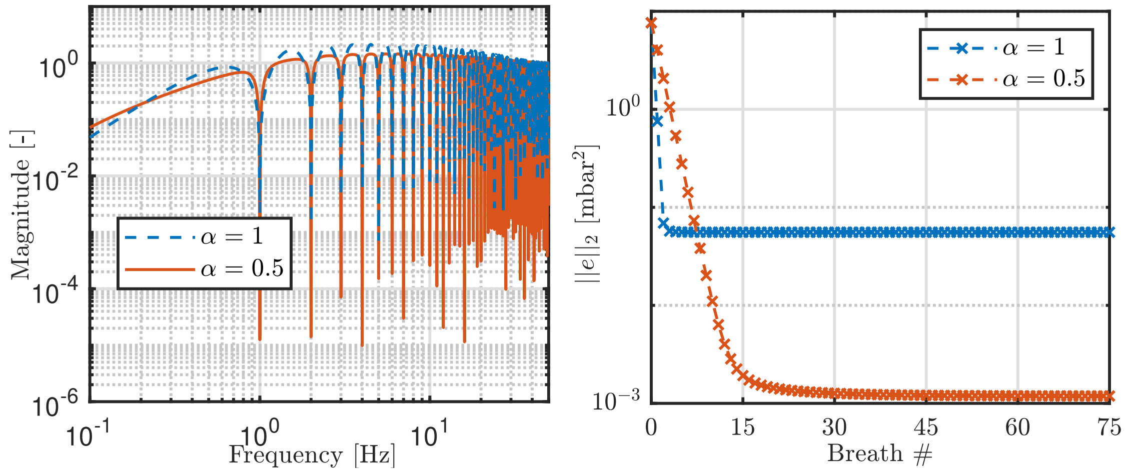

(a) Sensitivity $S_R S$ for a repetitive controlled system.

(b) Error norm of 75 breaths.

Figure 3.9. Influence of the learning gain α on the sensitivity $S_R S$ and error-norm of 75 breaths in the presence of aperiodic disturbances. The system used is the minimum phase system of Figure 3.7a.

3.4.2 Robustness filter design

This section describes the design methodology of the robustness filter Q. Throughout this section, the L-filter of Figure 3.7b is used. The previous section used a model of the complementary sensitivity T. In practice, however, this model is never exact or available. Therefore, in order to guarantee stability, Theorem 1 and 2 are typically used with a measured Frequency Response Function (FRF) of the complementary sensitivity T_{FRF}. Since the L-filter is based on a (possibly non-exact) model of T, Theorem 2 might be violated, i.e., $Q|(1 - T_{FRF}L)| \geq 1, \forall z = e^{i\omega}$ with $\omega \in [0, 2\pi)$ and $Q = 1$.
To guarantee stability, one typically chooses Q as a low-pass filter, with cut-off frequency f_{cut}, see Figure 3.11a. Hence, $Q \neq 1$ at frequencies above $\approx f_{cut}$. Then, by using (3.8), one can derive that the modified sensitivity $S_R \neq 0$ for the harmonics of the periodic disturbance above f_{cut}, see Figure 3.11a. From (3.7), it is observed that for $S_R \neq 0$, the tracking error $e \neq 0$. In other words, if $Q \neq 1$, the error 2-norm is non-zero after convergence, see Figure 3.11b. Thus, the tracking performance is lower compared to the case that $Q = 1$. However, if $Q \neq 1$, robustness is increased. Therefore, a performance vs. robustness trade-off exists in designing the robustness filter Q.

Typically, Q is a non-causal zero-phase Finite Impulse Response (FIR) filter, which is implemented by computing a causal FIR-filter Q and applying a forward shift of z^{p_q}. Therewith, Q is a zero-phase FIR-filter and, thus, no phase lag is introduced when filtering. See Figure 3.10 for an example Q_c and Q.
Since the control scheme already contains a buffer of length N, z^{-N}, it is possible to use non-causal L and Q, however, only for $p + d + p_q \leq N$. If this inequality is violated, one requires knowledge of future values of the tracking error e, which are not a priori known.

3.4.3 Repetitive control design procedure

In this section, a typical design procedure of a repetitive controller is given. First, the learning filter L is designed using ZPETC. For further details see Section 3.4.1. Thereafter, $|1 - T_{FRF}L|$ is used to check if stability is guaranteed using Theorem 2. If the closed-loop is asymptotically stable, the robustness filter Q can be unitary, which is advised if

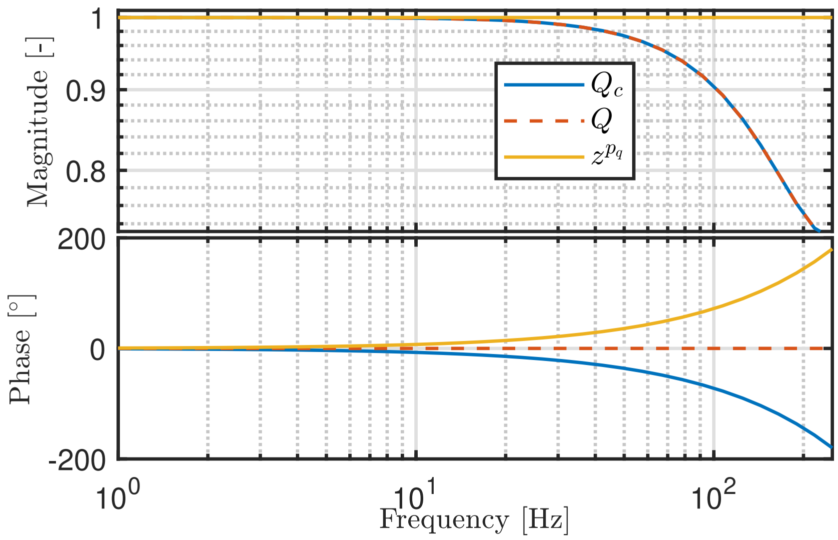

Figure 3.10. Example of a second-order causal FIR-filter Q_c and a non-causal zero-phase FIR-filter $Q = z^{p_q} Q_c$, where p_q is equal to half the filter order.

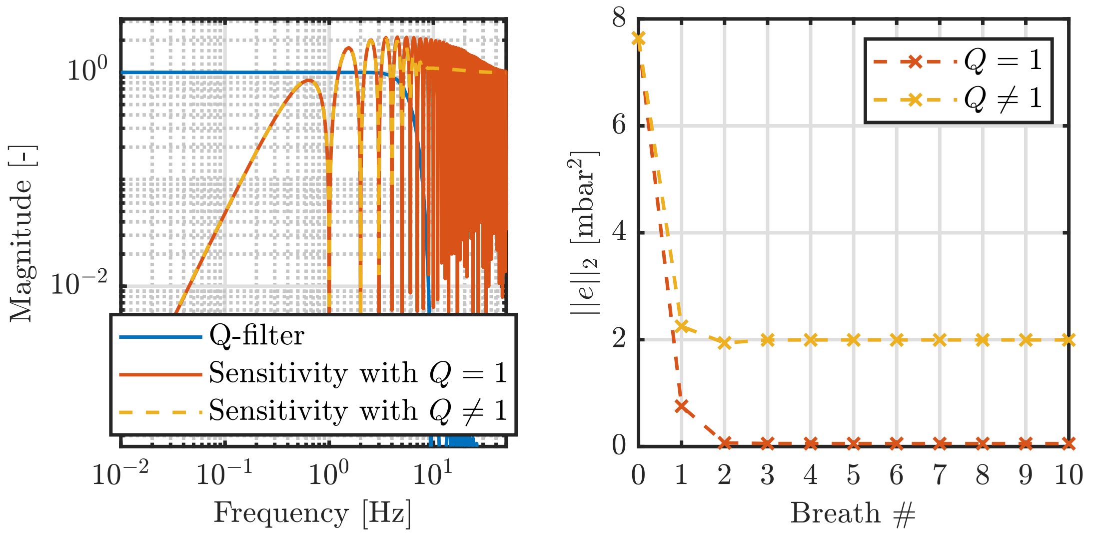

(a) Bode magnitude plots of the Q-filter and sensitivity with $Q = 1$ and with $Q \neq 1$.

(b) Error 2-norm with- and without a Q-filter.

Figure 3.11. Sensitivity and tracking error comparison compared for the case with- and without a Q-filter.

tuning for performance. See Section 3.4.2 for further details. If stability is not guaranteed, a robustness-filter Q is designed to guarantee stability using Theorem 2. An example of $|1 - T_{FRF}L|$ and $|Q(1 - T_{FRF}L)|$ are shown in Figure 3.12. It is seen that without Q-filter stability is not guaranteed, since $|1 - T_{FRF}L| \geq 1$ for some frequencies. However, when using a 50th-order FIR-filter with cut-off frequency of 23 Hz, it is seen stability is guaranteed, since $|Q(1 - T_{FRF}L)| < 1$ for all frequencies.

3.5 Summary

This chapter has described the repetitive control theory in detail. First, a brief comparison of ILC and repetitive control has been given. From this comparison, it followed

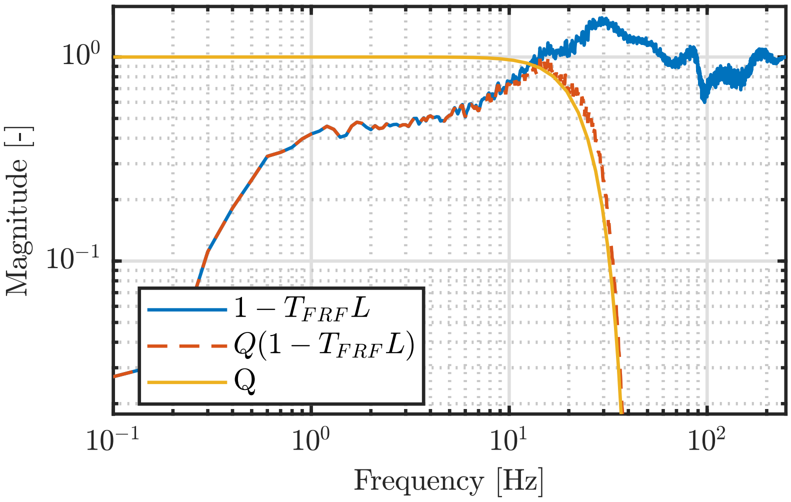

Figure 3.12. Bode magnitude plots of $1 - T_{FRF}L$ and $Q(1 - T_{FRF}L)$ to check if the closed-loop is asymptotically stable using Theorem 2.

that repetitive control should be used in application with mechanical ventilation instead of ILC. Thereafter, the basic principles of repetitive control have been treated. The internal model principle has been described and illustrative examples have been given. Thereafter, it has been shown how repetitive control is added upon an existing feedback control loop. Thereafter, a necessary and sufficient-, and a sufficient stability condition have been presented. Finally, it has been described how one can design a learning- and robustness filter to shape the repetitive controller, such that the stability, and required performance and robustness are obtained. It has been shown that if the learning-filter is not based on an exact model of the system, the error 2-norm convergence rate decreases. Furthermore, aperiodic disturbances are amplified by the repetitive controller. This amplification can be reduced by the use of a learning gain. Thereafter, it has been shown that if a robustness-filter is used, the error 2-norm upon convergence increases and, thus, performance decreases. However, robustness increases and, therefore, a performance vs. robustness trade-off exists in designing Q.

In the next chapter, the theory from this chapter is applied to mechanical ventilation in fully sedated patient scenarios.

Chapter 4

Repetitive Control Applied to Fully Sedated Patient Scenarios

This chapter describes the results of repetitive control applied to fully sedated patient scenarios. First, in Section 4.1, the measurement setup is described. Thereafter, in Section 4.2, the fully sedated patient scenario descriptions are presented. In Section 4.3, simulations on fully sedated patient scenarios are treated. Subsequently, in Section 4.4, the repetitive controller design procedure for experiments is described. Then, in Section 4.5, experiments on fully sedated patient scenarios are described. Finally, this chapter is summarized in Section 4.6.

4.1 Measurement setup

In this section, the measurement setup used in experiments is briefly described. In experiments, the breathing simulator shown in Figure 4.1 is used. A schematic of the measurement setup is shown in Figure 4.2. The hose is connected to the respiratory module and the ASL 5000 breathing simulator. Data from the respiratory module is send via dSPACE (dSpace Inc., Wixom, MI) to a computer in which the processing is done in Matlab (Mathworks, Natick, MA). The sampling frequency in the experiments is 500 Hz.

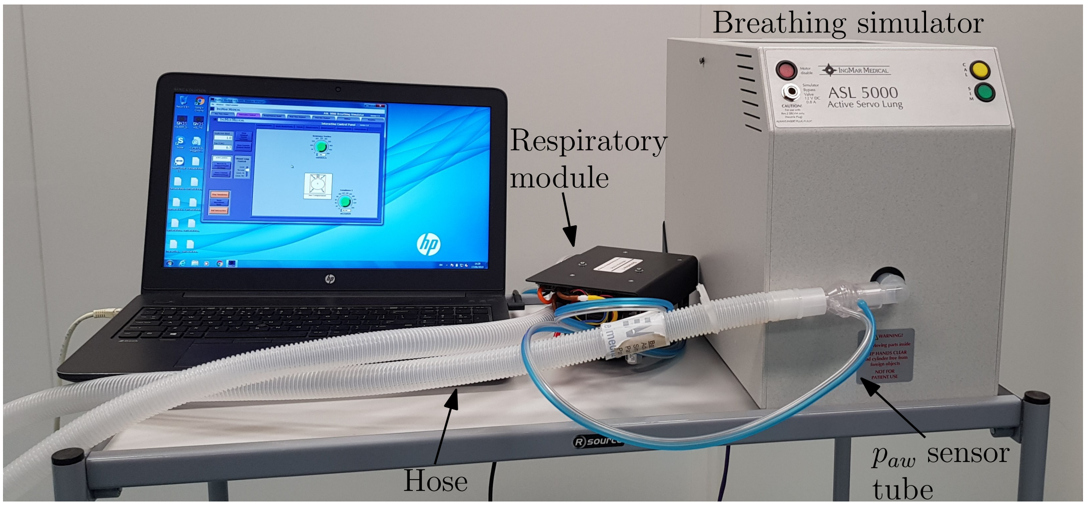

Figure 4.1. The ASL 5000 breathing simulator (IngMar Medical, Pittsburgh, PA) that is used in experiments to emulate a patient.

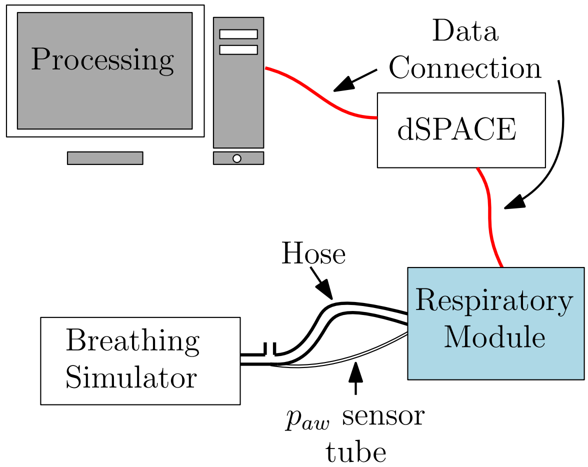

Figure 4.2. Schematic of the measurement setup.

Table 4.1. Patient-hose parameters and ventilation settings used in simulations and experiments for every scenario.

Parameter	**Adult**	**Pediatric**	**Baby**	**Unit**
R_{lin}	4.97	4.97	4.97	mbar s / L
R_{leak}	43.12	43.12	43.12	mbar s / L
R_{lung}	5	50	50	mbar s / L
C_{lung}	50	10	3	L/mbar $\cdot 10^{-3}$
Respiratory rate	15	20	30	breaths / min
PEEP	5	5	10	mbar
IPAP	15	35	25	mbar
Inspiratory time	1.5	1	0.6	s
Expiratory time	2.5	2	1.4	s

4.2 Fully sedated patient scenarios

This section presents the fully sedated patient scenarios considered in simulations and experiments. Since a mechanical ventilator is used on a variety of patients, simulations and experiments are done on several patient types. Each patient type has a different setting of the mechanical ventilator. A patient type with the corresponding settings of the mechanical ventilator are considered to be a scenario. The parameters used in simulations and experiments for the considered scenarios are given Table 4.1.
In Table 4.1, R_{leak} and R_{lin} are obtained by measurement. R_{leak} is defined as the leak resistance, R_{lin} is the hose resistance, R_{lung} is the resistance of the airway, and C_{lung} is the compliance of the lungs. For the definitions of PEEP (Positive End Expiratory Pressure), IPAP (Inspiratory Positive Airway Pressure), and the inspiratory- and expiratory times, see Figure 1.3.
The considered control strategies in the simulations and experiments are:

- Unit feedforward (FF), i.e., the feedforward signal is equal to the target pressure p_{target};
- Linear feedback (FB), with $C(z) = 6.285\frac{T_s}{2}\frac{z+1}{z-1}$ obtained via Tustin's method;
- Hose resistance compensation;
- Repetitive control.

In the former three an internal controller of the blower is used that ensures $p_{control} \approx p_{out}$ up 10 Hz. For more details see Section 1.2.1. Repetitive control contains unit feedforward and the linear feedback controller $C(z)$, but no internal controller of the blower. The

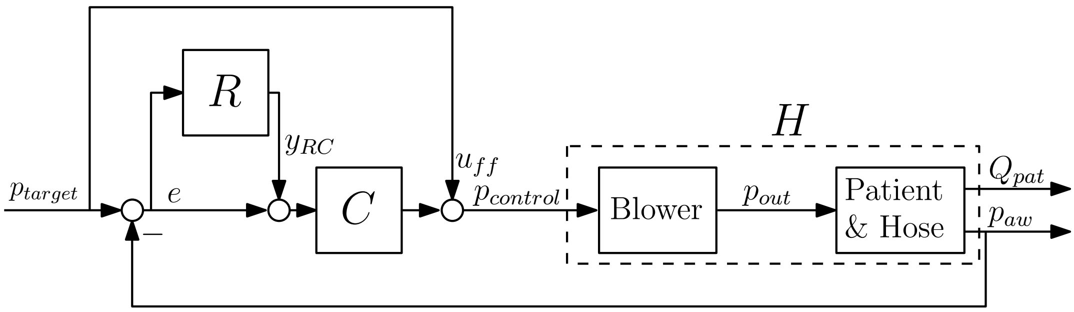

Figure 4.3. Control scheme for repetitive control applied to mechanical ventilation.

control scheme with repetitive control is given in Figure 4.3. In Chapter 3, repetitive control has been described in more detail.

4.3 Simulations on fully sedated patient scenarios

In this section, simulation results on fully sedated patient scenarios are presented. The simulations are conducted to show the possible tracking performance gain of repetitive control applied to fully sedated patient scenarios. The simulation results of all scenarios are similar, therefore, simulations of only one scenario are shown. In Section 4.3.1, it is described how the repetitive controller for mechanical ventilation in simulation is designed. Thereafter, in Section 4.3.2 simulation results are given. Note that in simulations the true system is equal to a zero-order hold discretized plant model (2.21) and no delays are included in the system.

4.3.1 Filter design for mechanical ventilation

This section describes how the repetitive controller is designed for mechanical ventilation. First, a learning filter is designed based on the plant model (2.21). Thereafter, a robustness filter is designed. In Figure 4.4a, the complementary sensitivity T of Figure 4.3 for $R = 0$, is given. The learning filter L is designed by using ZPETC, see Section 3.4.1. Figure 4.4b depicts the resulting causal- and non-causal L-filter, compared with the true complementary sensitivity inverse T^{-1}. It is seen that $|L| \neq |T^{-1}|$ for high frequencies. This mismatch is caused by T being non-minimum phase and, therewith, the learning filter L is approximately equal to T^{-1} as explained in Section 3.4.1.
In Figure 4.5, a Bode magnitude plot of $|Q(1 - TL)|$ with $Q = 1$, is shown. Using Theorem 2, it is concluded that the closed-loop is asymptotically stable. Hence, a unitary Q-filter yields an asymptotically stable closed-loop. This is as expected, since L was designed based on an exact model of the system T, i.e., the system used for simulations. Besides, the difference between $|L|$ and $|T^{-1}|$ due to T being non-minimum phase is small. In other words, the difference between the L-filter and the true inverse of the system T^{-1} is small and, therefore, a unitary Q-filter yields an asymptotically stable closed-loop.

4.3.2 Simulation results for fully sedated patient scenarios

This section presents the simulation results for fully sedated patient scenarios. The filters designed in the previous section are used in these simulations. In Figure 4.6, the tracking performance and error 2-norm are compared for the state-of-practice controllers and the repetitive controller. It is observed that the hose resistance compensation is the best state-of-practice controller in terms of tracking performance. However, the repetitive

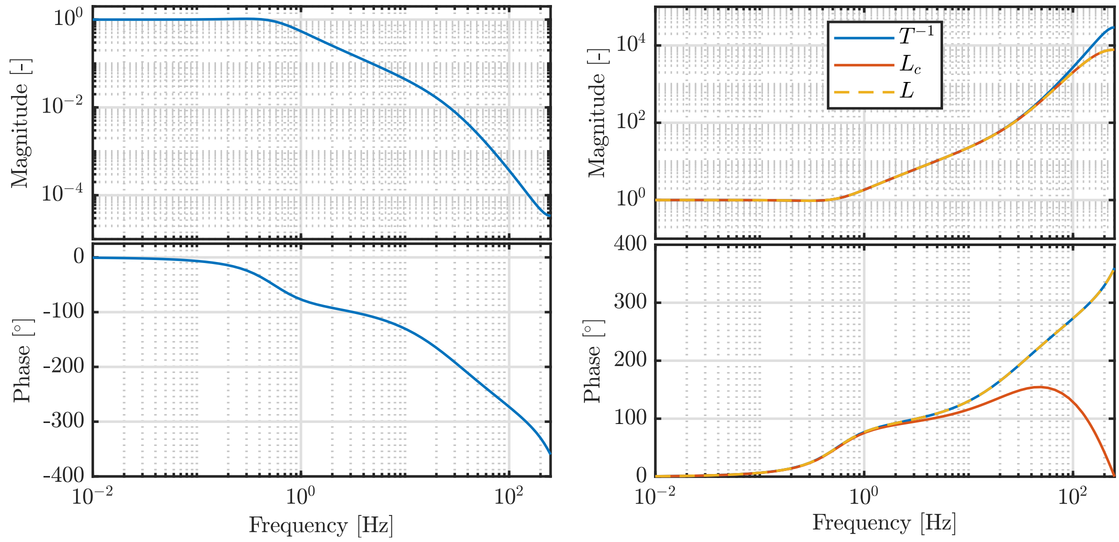

(a) Complementary sensitivity T of the model in Section 2.1.4.

(b) The inverse of T, and the causal- and non-causal L-filter designed with ZPETC.

Figure 4.4. Bode plots for repetitive control design in simulation.

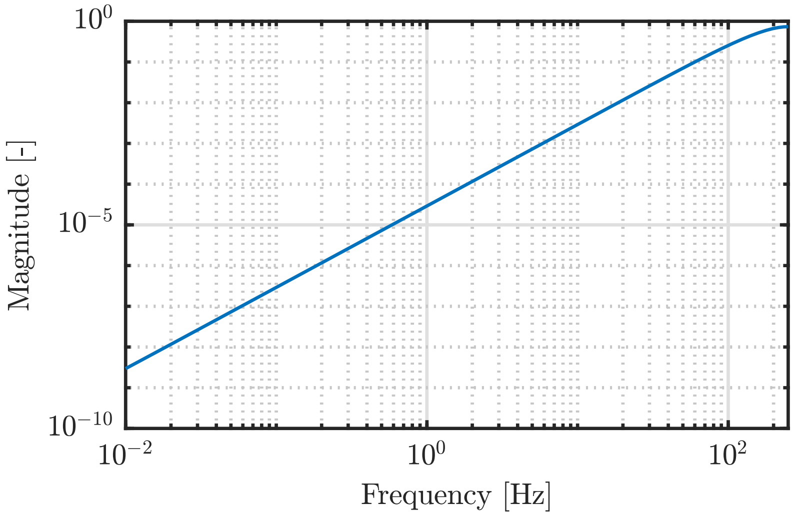

Figure 4.5. Bode magnitude plot of $Q(1 - TL)$.

controller has an even better tracking performance after convergence. The hose resistance compensation fully compensates the pressure drop caused by the hose and, thus, when assuming the blower dynamics as a unitary gain, perfect tracking is obtained. The blower dynamics are only a unitary gain for frequencies up to 10 Hz. In practice, however, p_{target} has some frequency content above 10 Hz. Therefore, when using hose resistance compensation without assuming blower dynamics as a unitary gain, an error remains, which is observed in Figure 4.6. Repetitive control includes the hose- and blower dynamics in learning. Since p_{target} is periodic, hence, it is asymptotically rejected by the repetitive controller, see Section 3.2.1. Therefore, the tracking performance of the repetitive controller is better than that of the state-of-practice controllers. In Figure 4.7, the error for five consecutive breaths is depicted for the linear feedback- and repetitive controller. It is observed that the repetitive controller, indeed, asymptotically rejects the periodic target pressure p_{target} and, thus the tracking error e reduces to zero.

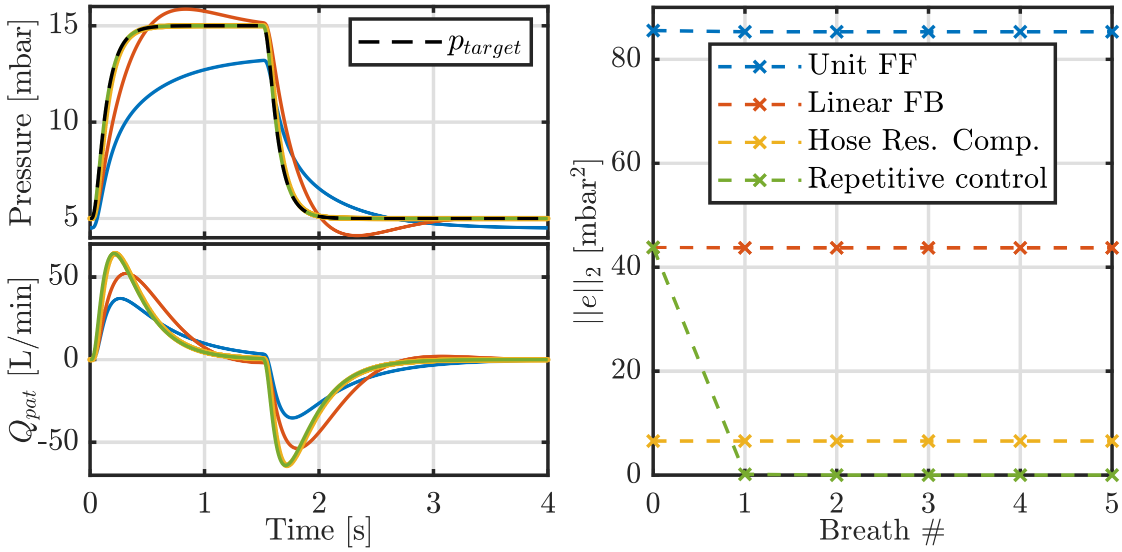

(a) Airway pressure p_{aw} and patient flow Q_{pat} after convergence of the repetitive controller (breath 5).

(b) Error 2-norm of five consecutive breaths.

Figure 4.6. State-of-practice controllers and repetitive control for the adult scenario in simulation.

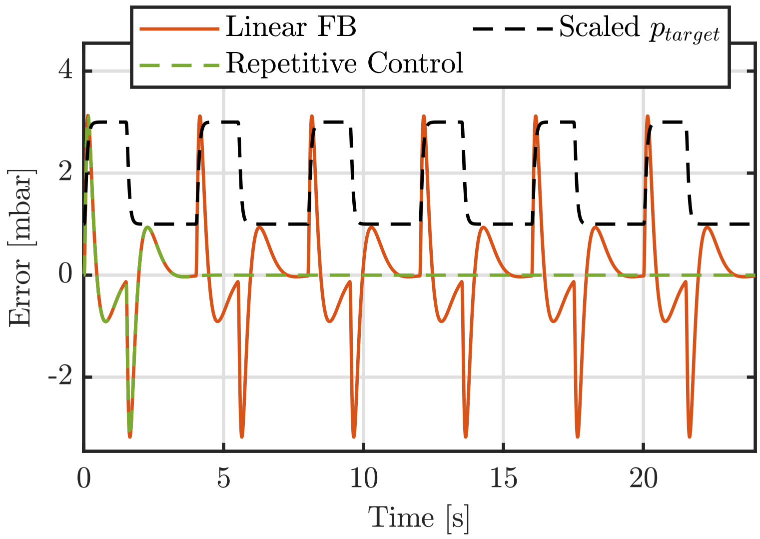

Figure 4.7. Tracking error e for five consecutive breaths for the adult scenario in simulation.

4.4 Repetitive control filter design for experiments

In this section, repetitive controller design for experiments is explained. The repetitive controller is designed such that it ensures closed-loop stability on a variety of patients. Different repetitive controller designs are considered. First, in Section 4.4.1, the repetitive controller is designed based on the first-principle model (2.21). Thereafter, in Section 4.4.2, a fit of an average FRF of the system is used to design the repetitive controller.

Table 4.2. Average patient parameters

Scenario	R_{lung} **[mbar s / L]**	C_{lung} **[L / mbar]** $\cdot 10^{-3}$
Adult	5	50
Pediatric	50	10
Baby	50	3
Average	35	21

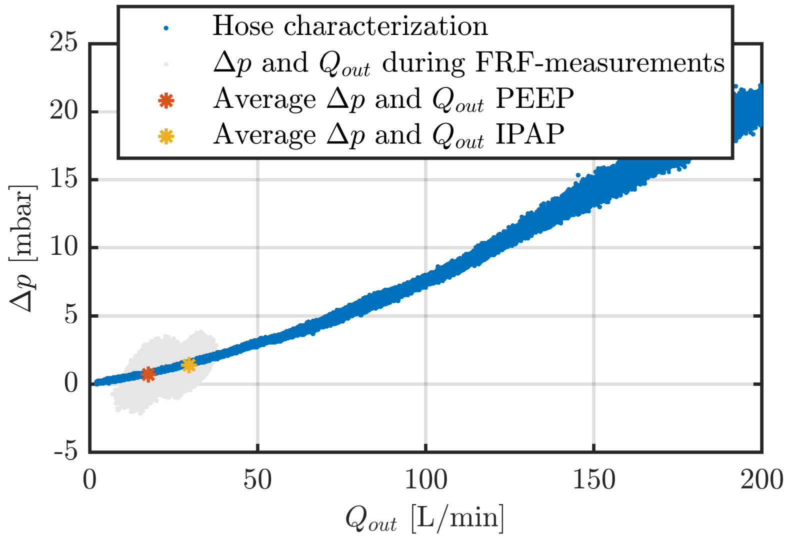

Figure 4.8. The average pressure drop over the hose Δp over the average output flow Q_{out} for both FRF-measurements compared to the hose characterization of Figure 2.4 for the adult scenario. The FRF-measurements are done with an average airway pressure p_{aw} of PEEP and IPAP.

4.4.1 Repetitive controller design based on a first-principle model

Here, the repetitive controller is designed based on a zero-order hold discretized version of the first-principle model (2.21). In (2.21), no delays are taken into account. However, the blower has an input delay of 8 ms. Additionally, in the patient-hose system, it takes time for the pressure propagates through the p_{aw} sensor tube. Therefore, an output delay of 16 ms is present in the patient-hose system. In this section, a repetitive controller is designed on (2.21) without and with delays taken into account. Since the repetitive controller is used on a variety of patients, the learning filter L is designed using the average patient parameters of the considered patients, see Table 4.2.

In order to compare the models to the true system, FRF-measurements are performed. In the modeling of Section 2.1.2, the hose resistance R_{lin} is assumed linear. In practice, however, the hose resistance is quadratic. To linearize the model, FRF-measurements are done at an average airway pressure of PEEP and IPAP, i.e., the maximum target pressures during ventilation. Also see Figure 4.8. In total six FRF-measurements are done, two per scenario. Using the response of all six T_{FRF}, an average FRF is computed.

In Figure 4.9, a Bode plot of the average FRF, and the complimentary sensitivity T without and with delays are shown. At frequencies below 7 Hz the models match the average FRF. However, at frequencies above 7 Hz, a significant difference in magnitude exist, since the models do not contain higher-order dynamics. The phase of the model with delays matches the phase of the average FRF accurately, whereas the model without delays does not.

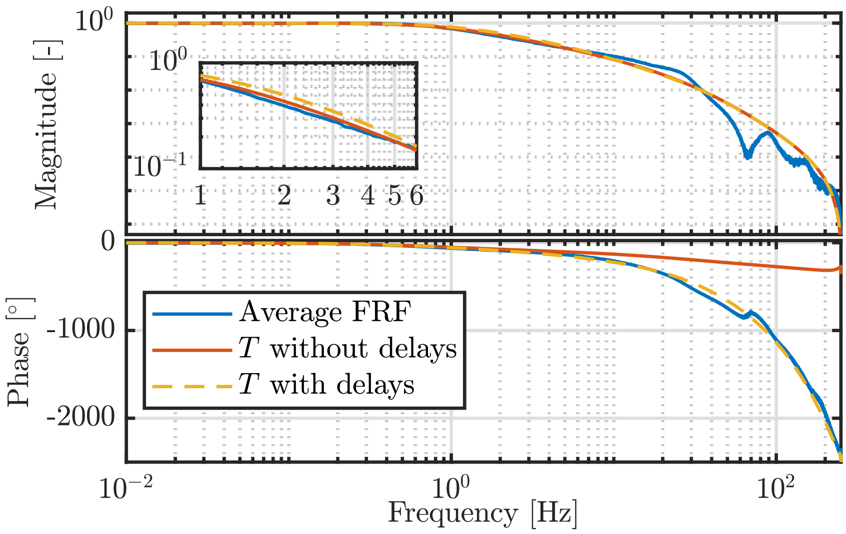

Figure 4.9. Complementary sensitivity of a model without and with delays, and an average of complimentary sensitivity FRF measurements for all scenarios. The magnitude difference in the zoom-plot between the model without and with delays is caused by internal delays, see Appendix A.

Using the models without and with delays, learning filters are designed. In Figure 4.10, the resulting non-causal L-filters are compared with the models. It is observed that a significant difference in phase exist between L based on the model without and with delays. This is as expected, since this phase difference is also present in the complimentary sensitivity T without and with delays. It is also observed that for high frequencies $|T^{-1}| \neq |L|$ for both the model without and with delays. This is due to the fact that the learning filter L is approximately equal to T^{-1}, since T is non-minimum phase, see Section 3.4.1.

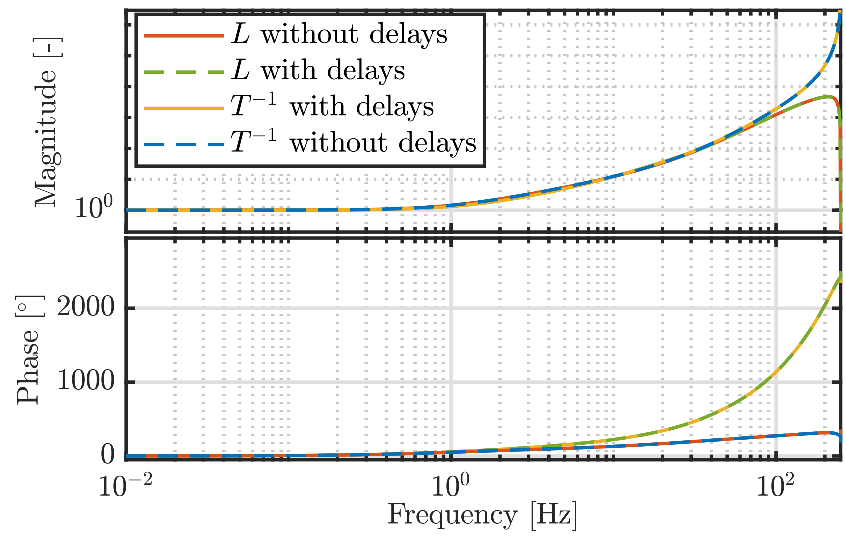

Figure 4.10. Comparison of T^{-1} and the non-causal L-filter based on a model with- or without delays.

To guarantee that the closed-loop system is asymptotically stable for both learning filters, two robustness filters Q are designed. This is done by computing $|(1 - T_{FRF}L)|$ for every T_{FRF} of all scenarios, i.e., not the average FRF, but all six T_{FRF} are used. A 50th-order low-pass FIR-filter is used as robustness filter Q and is tuned such that $|Q(1 - T_{FRF}L)|$ is just below 0 dB. In Figure 4.11, $|Q(1 - T_{FRF}L)|$ is depicted for every T_{FRF}, including the

Q-filters. The cut-off frequency of the robustness filters are 7.5 and 23 Hz for the learning filter L based on a model without and with delays, respectively. Thus, for L based on a model with delays, the cut-off frequency of Q is significantly higher compared to L based on a model without delays. This is as expected, since T with delays matches the average FRF significantly better than T without delays, i.e., the model quality of T with delays is better, see Figure 4.9. Due to a better model quality, $|T_{FRF}L|$ is closer to 1 for a broader range of frequencies, hence, $|1 - T_{FRF}L|$ is closer to zero for a broader range of frequencies. Thus, the cut-off frequency of Q can be increased, whilst guaranteeing closed-loop stability. In Figure 4.11 it is observed that for both L-filters, Theorem 2 is satisfied. Therefore, the closed-loops are asymptotically stable.

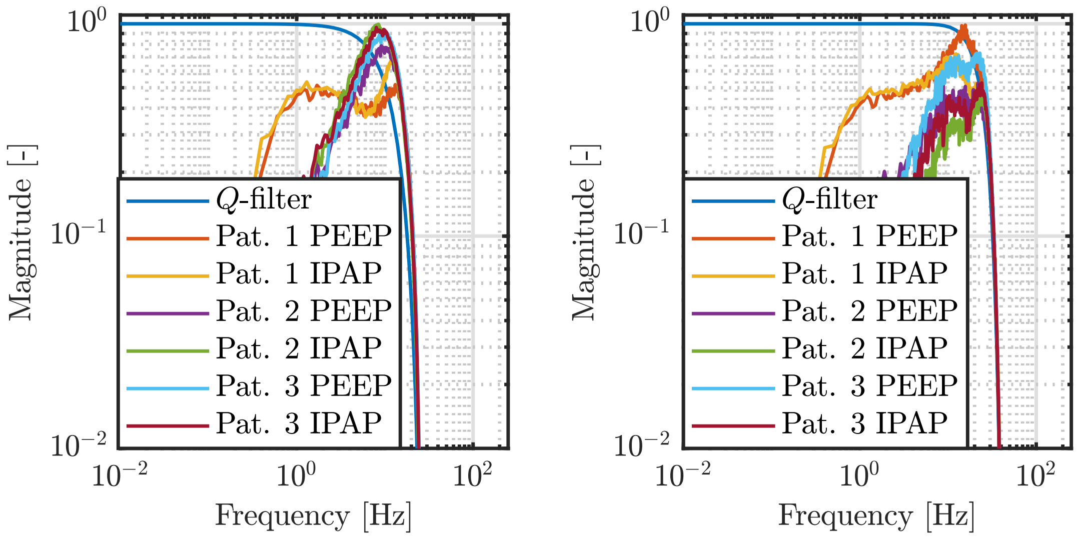

(a) With L-filter based on a model without delays (cut-off frequency 7.5 Hz).

(b) With L-filter based on a model with delays (cut-off frequency 23 Hz).

Figure 4.11. $|Q(1 - T_{FRF}L)|$ for a model based on a model without or with delays. T_{FRF} is measured and linearized for two average airway pressures per patient (PEEP and IPAP).

4.4.2 Repetitive controller design based on a fit of an average FRF

In this section, the repetitive controller is designed based on a fit of the average FRF. Similar to Section 4.4.1, the average FRF is computed using the response of all six T_{FRF}, two FRF's per scenario. All six FRF's are shown in Figure 4.12. The fit is fourth-order since a lower order fit decreases the quality of the fit with respect to the FRF significantly. However, a higher-order fit results in a fit of a single measurement. Since robustness with respect to plant variation is required, the order of the fit is not increased. In Figure 4.12, the complimentary sensitivity of the first-principle model with delays of Section 4.4.1, and a fourth-order fit T_{fit} of the average FRF are compared with the average FRF. It is observed that the fit matches the FRF significantly better, especially for frequencies above 7 Hz.

A learning filter L is designed based on T_{fit} using ZPETC. To guarantee closed-loop stability with this learning filter, two robustness filters Q are designed. Both Q-filters are 50th-order FIR-filters, however, the cut-off frequencies are different. The first Q-filter is tuned such that $|Q(1 - T_{FRF}L)|$ is as close to 0 dB as possible, resulting in a cut-off frequency of 54 Hz, see Figure 4.13a. The second Q-filter is tuned such that the maximum of $|Q(1 - T_{FRF}L)|$ is ≈ -5 dB, resulting in a cut-off frequency of 23 Hz, see Figure 4.13b. The latter is done to increase robustness of the controller with respect to plant variations.

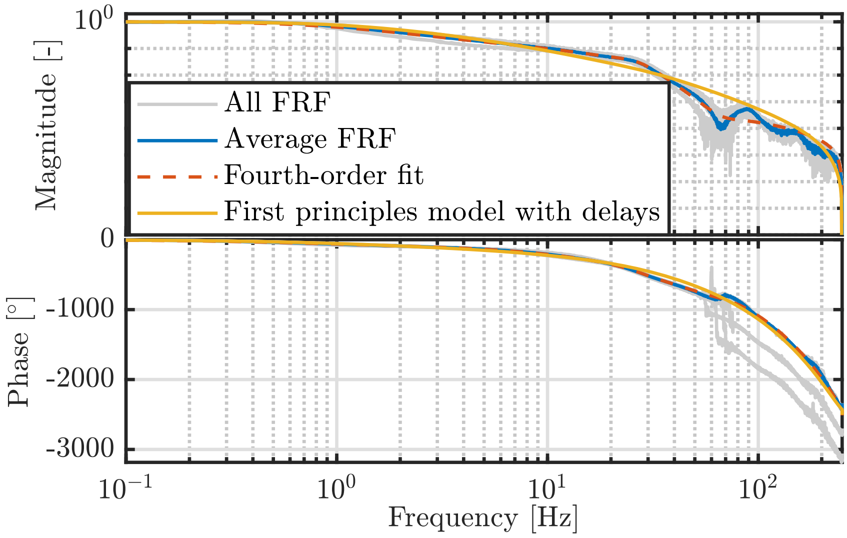

Figure 4.12. Complementary sensitivity of a model with delays, a fit on an average FRF and an average of complimentary sensitivity FRF measurements for all scenarios.

This robustness is particularly desired for mechanical ventilation, since a wide variety of patients is ventilated. In Figure 4.13, it is seen that Theorem 2 is satisfied for both Q-filters and, thus, the closed-loops are asymptotically stable.

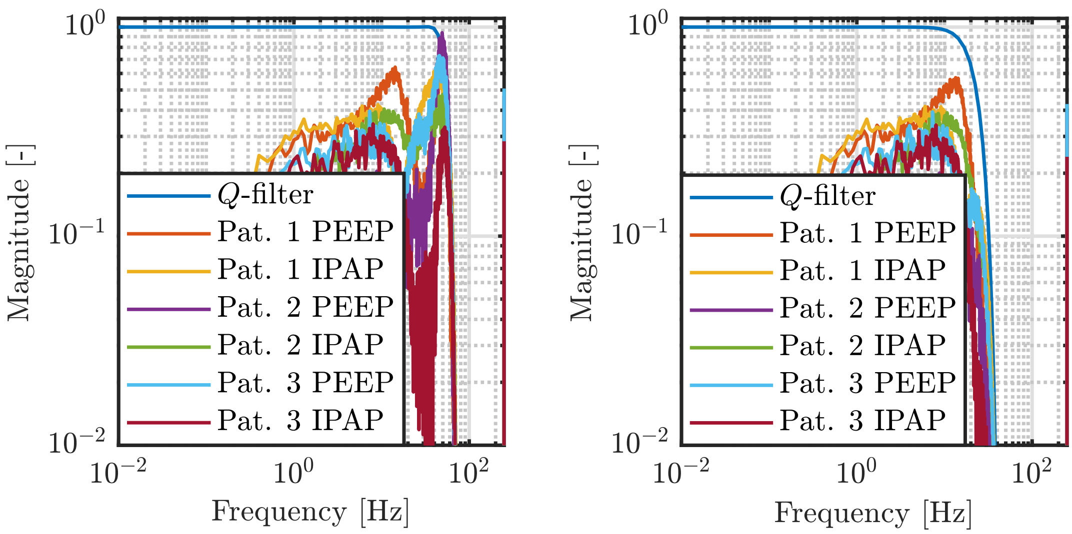

(a) With L-filter based on a fit and a high cut-off frequency (54 Hz) for Q.

(b) With L-filter based on a fit and a low cut-off frequency (23 Hz) for Q.

Figure 4.13. $|Q(1 - T_{FRF}L)|$ for L based on a fit of an average FRF for two different Q-filters. T_{FRF} is measured and linearized for two average airway pressures per patient (PEEP and IPAP).

4.5 Experiments on fully sedated patient scenarios

This section describes the experimental results of the fully sedated patient scenarios. First, in Section 4.5.1, a comparison between all four repetitive controllers, designed in previous section, is made. Thereafter, in Section 4.5.2, the state-of-practice control strategies, described in Section 1.2.1, are compared with repetitive control. In all experiments

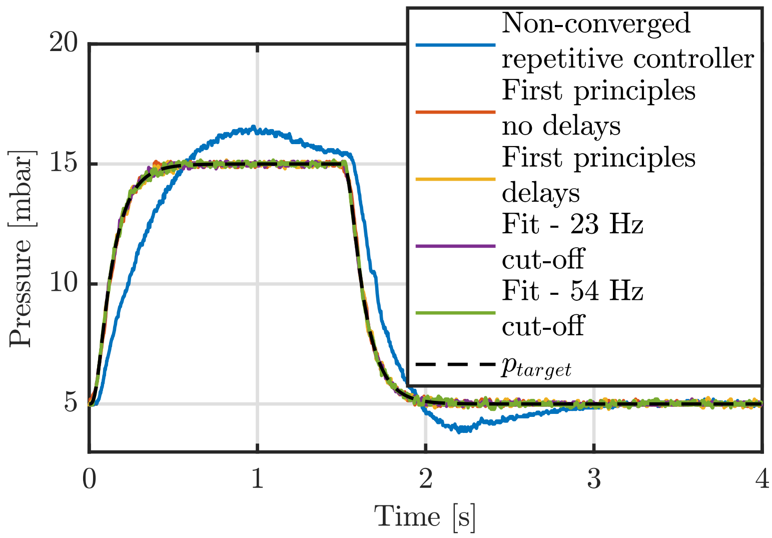

Figure 4.14. Tracking performance and error 2-norm before- and after convergence of repetitive control for the adult scenario in experiments.

the ASL 5000 breathing simulator (IngMar Medical, Pitssburgh, PA) is used, to emulate the patient.

4.5.1 Comparison of different repetitive controllers

In this section, all four repetitive controllers designed in Section 4.4 are compared. The main difference between the repetitive controllers of Section 4.4 how good the model, on which the repetitive controllers are based, matches the true system. In this section, a recommendation is made on which repetitive controller should be used in practice. In Figure 4.14 different repetitive controllers are compared. Also, p_{aw} for the case where the repetitive controllers have not start learning yet is included. It is observed that all repetitive controllers significantly improve the tracking performance in terms of rise- and fall-time, and over- and undershoot compared to the non-converged breath. However, no clear difference between the repetitive controllers is observed from Figure 4.14.
In Figure 4.15, the error 2-norm is shown for all four repetitive controllers designed in Section 4.4. Also, a lower bound on the error 2-norm is shown in Figure 4.15. This lower bound is computed by predicting the performance that can be achieved when applying repetitive control. For this prediction, the methodology given in [20] is used. First, N_{exp} experiments without repetitive control are done, while the error for every breath, $e_j, j = 0, ..., N_{exp} - 1$, is measured. Thereafter, the sample-mean $m_e(k)$ is computed:

$$m_e(k) = \frac{1}{N_{exp}} \sum_{j=0}^{N_{exp}} e_j(k), \tag{4.1}$$

where $k \in \mathbb{Z}$. Repetitive control is able to compensate for $m_e(k)$, i.e., the periodic part of the tracking error e. The maximal achievable performance after learning, i.e., the residual error or the aperiodic part of the tracking error e, is given as: $e_j(k) - m_e(k), j = 0, ..., N_{exp} - 1$. A repetitive controller rejects periodic disturbances, however, e also has an aperiodic part, which is not rejected by the repetitive controller. Therefore, the aperiodic part of e represents the maximal achievable performance after a repetitive controller

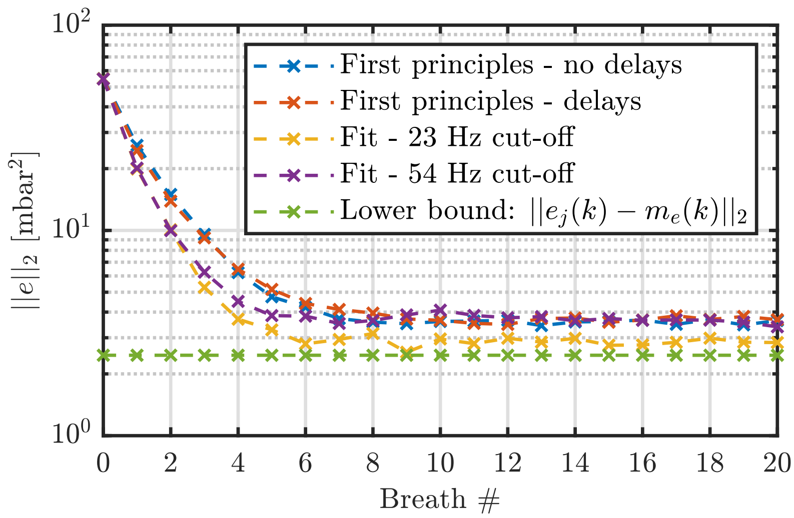

Figure 4.15. Error 2-norm for different repetitive controllers and the lower-bound on the error 2-norm, for the adult scenario in experiments.

Table 4.3. Average error 2-norm of last ten breaths and lower-bound of the error 2-norm for all repetitive controllers and scenarios.

	First-principle no delays [mbar^2]	**First-principle delays [mbar^2]**	**Fit 23 Hz [mbar^2]**	**Fit 54 Hz [mbar^2]**	$\|\|e_j - m_e\|\|_2$ **[mbar^2]**
Adult	3.58	3.67	2.87	3.67	2.47
Pediatric	5.83	2.92	2.84	3.00	2.21
Baby	3.35	2.35	2.21	2.55	1.69
Average	4.25	2.98	2.64	3.07	-

has learned the periodic part of e. Thus, by computing $||e_j(k) - m_e(k)||_2$, a lower-bound on the error 2-norm for repetitive control is obtained.

Figure 4.15 shows that the convergence rate for the repetitive controllers based on fit compared to the repetitive controllers based on a first principle model, is slightly higher. This is as expected, since Section 4.4.2 already concluded that the fit matches the FRF significantly better than the first principle models. Therefore, the learning filter based on a fit approximates the true inverse of the system better and, hence, the convergence rate is higher, see Section 3.4.1. In Table 4.3, the average error 2-norm of the last ten breaths and $||e_j(k) - m_e(k)||_2$, is given for all repetitive controllers and different scenarios.

Table 4.3 shows that the repetitive controllers based on the fit result in a significant difference in error 2-norm. However, based on Section 3.4.2, for a higher cut-off frequency of the Q-filter one expects a decrease in the error 2-norm. However, the higher cut-off of the robustness filter Q results in an increase in error 2-norm. This phenomenon can be explained by considering the power spectral density (PSD) of the periodic and and aperiodic disturbances. In Figure 4.16, the PSD of $e_j(k) - m_e(k)$ and $m_e(k)$ are shown for an adult, including the locations of the cut-off frequencies for every Q-filter. For the adult, it is observed that, $e_j(k) - m_e(k)$ has a higher power than $m_e(k)$ for frequencies above 23 Hz. Hence, for the Q-filter with a cut-off frequency of 54 Hz, the repetitive controller controller amplifies the aperiodic part of the disturbance more compared to the Q-filter wit a 23 Hz cut-off frequency. Since repetitive control amplifies aperiodic disturbances, see Section 3.4.1, a higher error 2-norm results upon convergence for the Q-filter with a cut-off frequency of 54 Hz.

In Table 4.3, the lowest average error 2-norm for every scenario is achieved with the

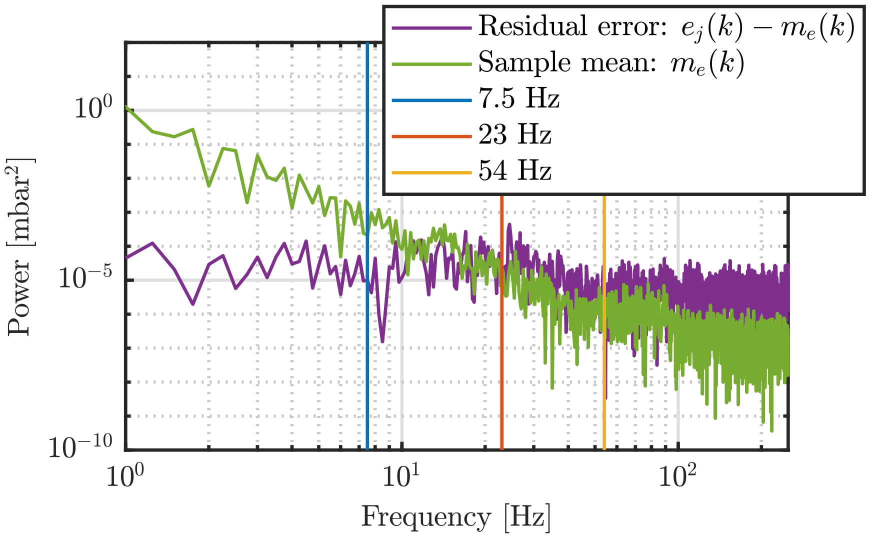

Figure 4.16. Power spectral density of the sample mean of the error, $m_e(k)$, and residual error after learning, $e_j(k) - m_e(k)$, compared to different cut-off frequencies of the Q-filter for the adult scenario.

Table 4.4. Average error 2-norm of last ten breaths for state-of-practice and repetitive controller for every scenario in experiments.

	Unit feedforward [mbar^2]	**Linear feedback [mbar^2]**	**Hose resistance compensation [mbar^2]**	**Repetitive control [mbar^2]**
Adult	78.96	34.62	35.72	2.87
Pediatric	85.61	40.35	42.92	2.84
Baby	51.56	17.78	21.17	2.21

repetitive controller based on the fit with a cut-off frequency of 23 Hz for the Q-filter. Also, Section 4.4.2 describes that this repetitive controller has more robustness with respect to plant variations, compared to the other repetitive controllers. Therefore, it is recommended to use the repetitive controller based on the FRF fit with the robustness filter cut-off at 23 Hz.

4.5.2 State-of-practice control compared to repetitive control

This section gives a comparison of the state-of-practice control strategies, see Section 1.2.1, and the repetitive controller based on the fit with Q-filter with a cut-off frequency of 23 Hz, see Section 4.5.1. The focus in this section is on comparing the tracking performance of the state-of-practice controllers to the best repetitive controller.

In Figures 4.17, the tracking performance and error 2-norm of the state-of-practice control strategies and repetitive controller are depicted in an experiment of the adult scenario. The figure shows that repetitive control significantly improves the tracking performance compared to the state-of-practice control strategies. It is complex to obtain a good rise- and fall-time, and low over- and undershoot for the state-of-practice controllers, since a higher rise-time typically increases the overshoot for the (linear) feedback controllers. However, the repetitive controller succeeds in having a significant better rise- and fall-time, and low over- and undershoot. It is also observed that no overshoot occurs in the patient flow Q_{pat} for the repetitive controller.

In Table 4.4, the average error 2-norm is given for the state-of-practice controllers and repetitive control for every scenario. It is observed that the repetitive controller outperforms the state-of-practice controllers significantly with respect to tracking performance.

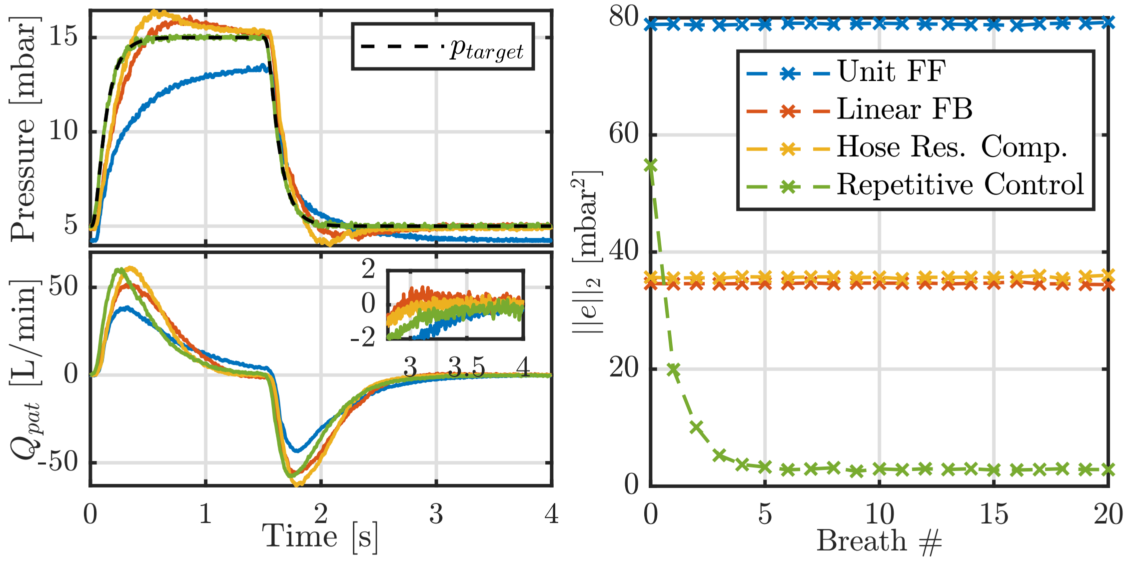

(a) Airway pressure p_{aw} and patient flow Q_{pat} after convergence of the repetitive controller (breath 20).

(b) Error 2-norm of 20 breaths.

Figure 4.17. State-of-practice control and repetitive control for the adult scenario in experiments.

4.6 Summary

In this chapter, repetitive control has been applied to fully sedated patient scenarios. First, the measurement setup has briefly been described. Second, the fully sedated patient scenarios have been defined. To show the working principle of repetitive control applied to fully sedated patient scenarios, simulations have been done. Thereafter, several repetitive controller designs have been discussed. Using these repetitive controllers, experiments have been conducted. A comparison based on tracking performance and robustness of each repetitive controller has been presented. One repetitive controller has been chosen to be used in further analysis. Thereafter, this repetitive controller has been compared to the state-of-practice controllers. This comparison has shown that repetitive control increases the tracking performance significantly for every fully sedated patient scenario.

Chapter 5

Repetitive Control Applied to Spontaneously Breathing Patient Scenarios

This chapter describes the results of repetitive control applied to spontaneously breathing patient scenarios. In Chapter 4, fully sedated patients are considered. Although a large population of patients is fully sedated, another large population of patients is not; they can breathe spontaneously. In Section 5.1, challenging scenarios for repetitive control applied to mechanical ventilation are identified. Thereafter, in Section 5.2, scenarios considered in this chapter are described in more detail. Then, the simulation- and experimental results of repetitive control applied to these scenarios are presented in Section 5.3 and 5.4, respectively. Finally, this chapter is summarized in Section 5.5. Throughout this chapter, the patient-hose parameters and ventilation settings of the adult scenario of Chapter 4 are used, see Table 4.1. Additionally, the same measurement setup is used in experiments, see Section 4.1.

5.1 Challenging scenarios for repetitive control applied to mechanical ventilation

In this section, challenging scenarios for repetitive control applied to mechanical ventilation are described. For fully sedated patient scenarios, repetitive control achieves significantly better tracking performance than the state-of-practice controllers, as shown in Chapter 4. In the fully sedated patient scenarios the following assumptions are made:

- the periodic target pressure profile p_{target} does not vary during ventilation;
- the patient does not breathe spontaneously.

In practice, however, the pressure profile p_{target} can change during ventilation, i.e., when a physician changes settings. Furtheremore, a patient often breathes spontaneously, i.e., when he/she is not fully sedated. Therefore, in this section, scenarios are presented in which these assumptions do not hold. Also, the challenges for repetitive control that are introduced by relaxing these assumptions are described. First, in Section 5.1.1, the challenges for repetitive control applied to mechanical ventilation with a change in target pressure profile are presented. Thereafter, the challenges for repetitive controlled ventilation of a spontaneously breathing patient are described in Section 5.1.2.

5.1.1 Target pressure variation scenario

If a physician changes the settings of the mechanical ventilator, the target pressure p_{target} changes. This is considered an aperiodic disturbance in repetitive control. The following settings are typically changed by a physician, also see Figure 5.1:

- PEEP or IPAP, i.e., the pressure plateaus during in- or expiration, respectively;

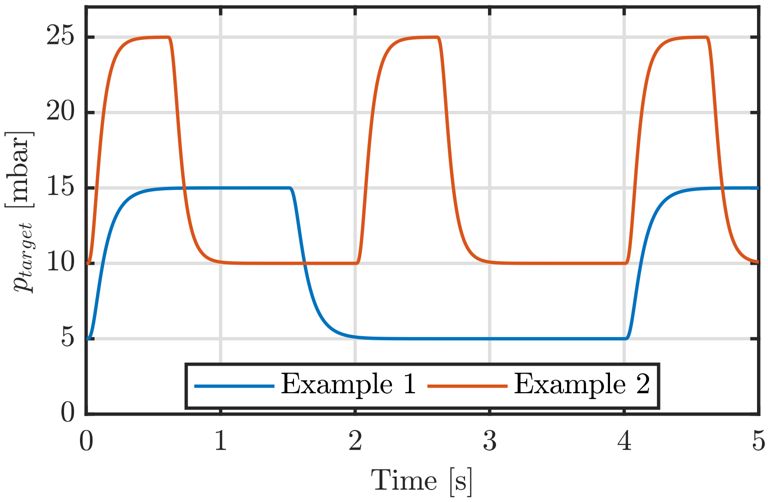

Figure 5.1. Two examples of target pressures p_{target}.

- Respiratory rate, i.e., the amount of breaths per minute;
- The ratio between the inspiratory time and the expiratory time;
- Rise- and fall-time, i.e., the time it takes for pressure to rise from PEEP to IPAP or to fall from IPAP to PEEP, respectively.

The challenge for repetitive control with a changing target pressure p_{target}, is that the resulting error due to the new target pressure and, therewith, input to compensate this error, are not learned by the repetitive controller yet. In other words, the internal model learned by the repetitive controller is significantly different than the disturbance generating system, see Section 3.2.1. Therefore, the tracking performance decreases significantly. A solution to this challenge is to reset the repetitive controller after a target pressure variation has occurred. Therewith, the repetitive controller restarts the learning process for the new target pressure. In Section 4.5.2, it is shown that the error 2-norm converges in approximately six breaths for the considered scenarios. These six breaths of converging are considered negligible compared to the typical 700-900 breaths per hour of a mechanical ventilator for the considered patients. Therefore, no further research is done in to the challenge for repetitive control due to a target pressure variation of the mechanical ventilator. It is recommended to reset the repetitive controller and restart the learning process.

5.1.2 Spontaneously breathing patient scenarios

This section describes the challenges for repetitive control if a patient is allowed to breathe spontaneously, i.e., patient effort is included in ventilation. For spontaneously breathing patients, ventilation modes that use triggering to synchronize the mechanical ventilator to the patient's respiratory rate are used. The most common mode of triggering is using patient flow triggers. A pressure controlled ventilator triggers if the patient flow Q_{pat} exceeds a physician-set threshold, a typical threshold for an adult is 2 L/min. With such a trigger, the mechanical ventilator determines when to start or stop in- and/or expiration. Spontaneous breaths are a result of a change in muscle activity of the patient, e.g., contraction of the diaphragm. The pressure induced by the muscles of the patient is defined as the patient effort p_{mus}. Due to patient effort, the lung pressure p_{lung} is changed.

For spontanenously breathing patients many different scenarios exist. It is assumed that a spontaneously breathing patient scenario consists of the following three main elements, which all have two options:

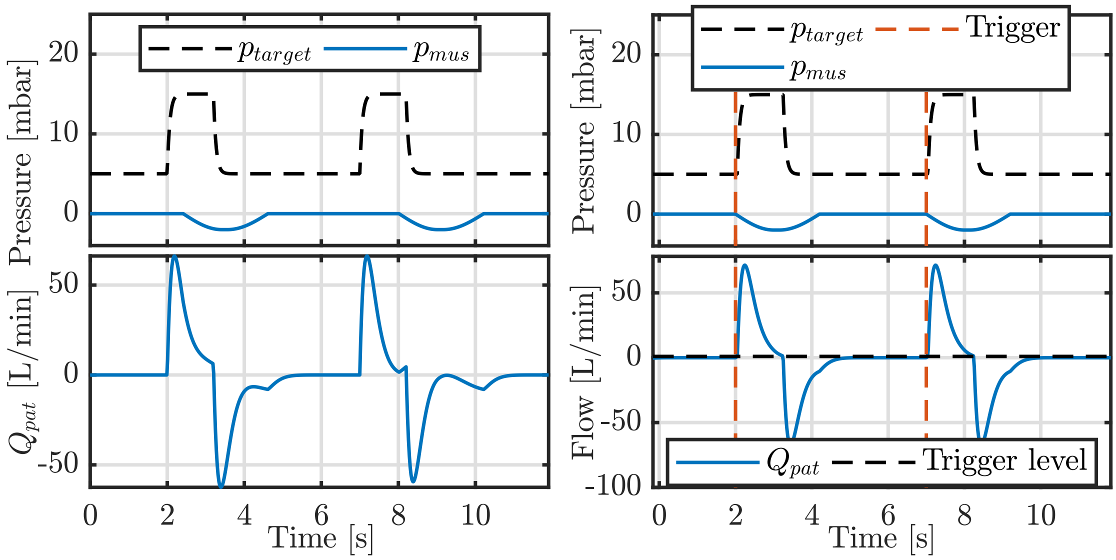

(a) Untriggered mechanical ventilation.

(b) Triggered mechanical ventilation.

Figure 5.2. Examples of different forms of mechanical ventilation with periodic patient effort that is constant in size for each breath.

1. **Ventilation mode:**
   (a) without triggering.
   (b) with triggering.
2. **Patient effort timing:**
   (a) periodic, i.e., the same length for each spontaneous breath such that the period length of the mechanical ventilator is an integer multiple of the length of a spontaneous breath.
   (b) aperiodic, i.e., a different length for each spontaneous breath.
3. **Patient effort amplitude:**
   (a) constant for each breath.
   (b) changes randomly, within certain bounds, for each breath.

A total of 8 possible combinations, i.e., scenarios, exist. See Figure 5.2a and 5.2b for examples of triggered- and untriggered mechanical ventilation, respectively. Next, a distinction is made between the scenarios for ventilation modes without and with triggering. This distinction is made, since the scenarios without triggering consider only the influence of the patient effort on the pressure tracking, while the target pressure p_{target} does not change. The scenarios with triggering, however, also consider a change in the target pressure p_{target} due to triggering.

In mechanical ventilation **without triggering**, the target pressure p_{target} is periodic. However, the spontaneous breaths of the patient introduce an unknown (possibly) aperiodic disturbance p_{mus} to the system. The challenge for repetitive control lies in the fact that p_{mus} is possibly aperiodic. As explained in Section 3.4.1, aperiodic disturbances are often amplified by the repetitive controller, decreasing the tracking performance. In Section 5.2, mechanical ventilation without a triggered mode is discussed in more detail.

In mechanical ventilation **with triggering**, the start of inspiration and expiration are determined by a trigger. Therewith, the timing of p_{target} is unknown and possibly varying for each breath. Hence, it can not be assumed that p_{target} is periodic for each breath. The latter decreases the tracking performance, as explained in the previous paragraph.

For ventilation modes with triggering, the disturbance p_{mus} is also present in the system. Hence, the challenge that exist for ventilation modes without triggering, also exist for ventilation modes with triggering. In this thesis, only ventilation modes without triggering are considered, see Section 5.2. Therefore, no further research is done in the challenges for repetitive control applied to triggered mechanical ventilation.

5.2 Considered spontaneously breathing patient scenarios

This section describes the spontaneously breathing patient scenarios that are considered in this chapter. As stated in previous section, only ventilation without triggering is considered. The following three scenarios for ventilation of spontaneously breathing patients are considered:

1. **Periodic scenario**, in which the spontaneous breaths have the same respiratory rate and amplitude for each breath. Also, the respiratory rate is the same as the mechanical ventilator. The results on this scenario are presented in Sections 5.3.1 and 5.4.1.
2. **Periodic scenario with a deep breath**, which is the same as the first scenario, however, every sixth breath is a "deep" breath. During this deep breath, the patient effort p_{mus} increases by 30 % in amplitude. The results on this scenario are presented in Sections 5.3.2 and 5.4.2.
3. **Aperiodic scenario**, in which the spontaneous breaths have a different respiratory rate (random between 12-15 breaths/min), but a constant amplitude for each breath. The results on this scenario are presented in Sections 5.3.3 and 5.4.3.

For all these scenarios, the tracking performance of the state-of-practice control strategies and repetitive control are compared in a simulation and experimental case-study, see Section 5.3 and 5.4, respectively.

In Table 5.1, the parameters of the patient effort are given for each scenario. The percentage are given as a percentage of the time of a full respiratory cycle. In Figure 5.3, the patient effort p_{mus} profile and corresponding target pressure is shown for each scenario.

Table 5.1. Patient effort parameters for each scenario.

Parameter	Periodic	Deep breath	Aperiodic
Respiratory rate [breaths/min]	15	15	12-15
Pressure rise % [-]	15	5	5
Pressure fall % [-]	5	5	5
Constant pressure % [-]	0	0	0
Amplitude [mbar]	6	6 or 7.8	6

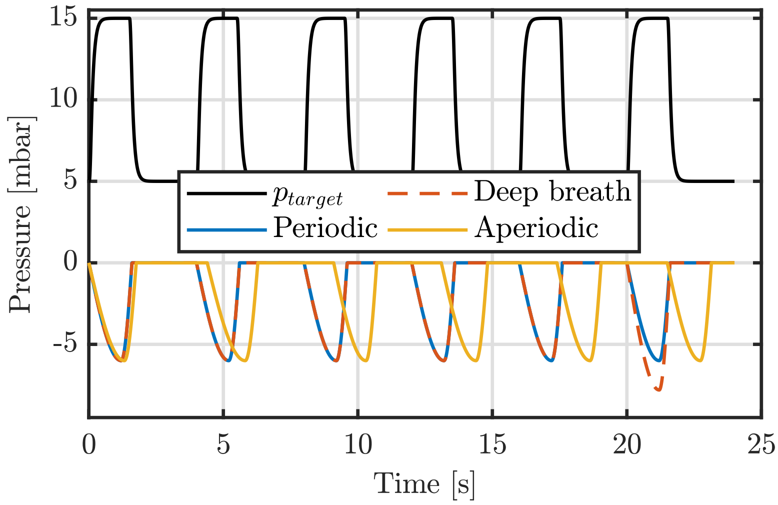

Figure 5.3. Patient effort profiles for each scenario.

The state-space defined in Section 2.1.4, including the disturbance p_{mus}, is given as follows.

$$\begin{aligned} \dot{x} = \begin{bmatrix} \dot{x}_b \\ \dot{p}_{lung} \end{bmatrix} &= A \begin{bmatrix} x_b \\ p_{lung} \end{bmatrix} + Bp_{control} + \dot{p}_{mus}, \\ y = \begin{bmatrix} p_{aw} & Q_{pat} \end{bmatrix} &= C \begin{bmatrix} x_b \\ p_{lung} \end{bmatrix}. \end{aligned} \tag{5.1}$$

Consider p_{lung} as the solution to (5.1). Then, p_{mus} influences the lung pressure p_{lung}. The lung pressure p_{lung} and airway pressure p_{aw} are directly related via (2.12). Therefore, the disturbance p_{mus} directly affects the airway pressure p_{aw}.

5.3 Simulations of spontaneously breathing scenarios

In this section, the simulation results of spontaneously breathing scenarios are presented. These results are used to compare the state-of-practice controllers with the repetitive controller from Section 4.3.1 in simulations. In simulations, an L-filter designed based on an exact model of the true system, i.e., the system used for simulations, and a unitary Q-filter are used. Also, a breathing simulator based on the ASL 5000 breathing simulator (IngMar Medical, Pitssburgh, PA), i.e., the breathing simulator used in experiments, is used to obtain different patient effort p_{mus} profiles. First, in Section 5.3.1, the periodic scenario is discussed. Thereafter, in Section 5.3.2, the periodic scenario with a deep breath scenario is discussed. Finally, the aperiodic scenario is discussed in Section 5.3.3.

5.3.1 Simulations of the periodic scenario

Here, the simulation results of the periodic scenario are presented and discussed. In Figure 5.4, the airway pressure and patient flow of the last breath, and the error 2-norm for all 25 breaths is given for the state-of-practice controllers and repetitive controller. It is observed that the repetitive controller has significant better tracking performance than the state-of-practice control strategies. This is as expected, since the same conclusion is drawn in Section 4.3.2 and, in this section, the only difference is that a periodic disturbance is injected in the system. The periodic disturbance has the same period as the buffer of the repetitive controller and, therefore, is rejected by the repetitive controller.

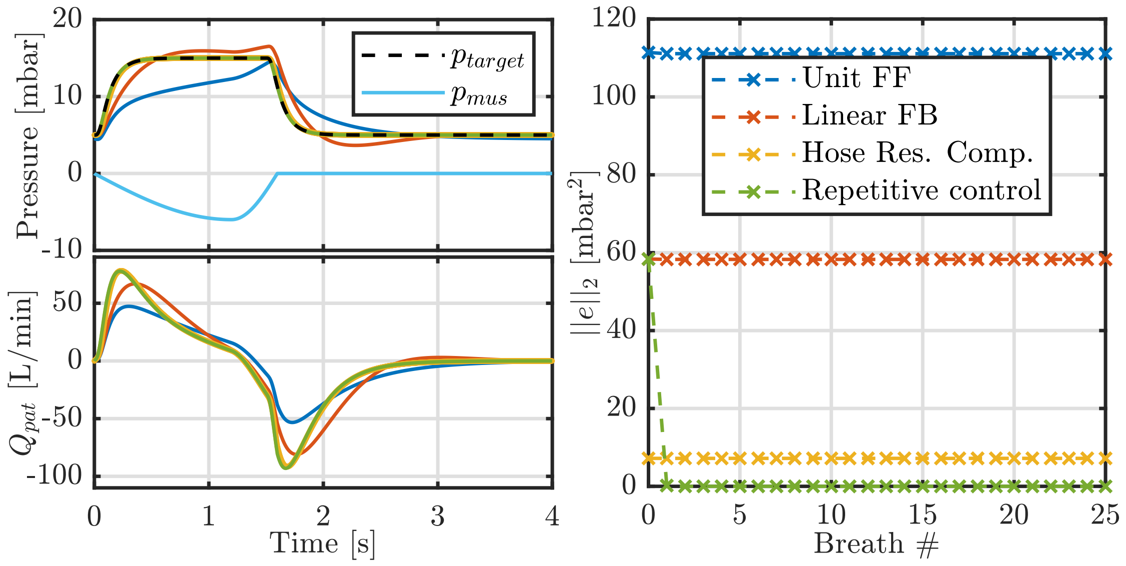

(a) Airway pressure p_{aw} and patient flow Q_{pat} after convergence of the repetitive controller (breath 25).

(b) Error 2-norm of 25 breaths.

Figure 5.4. State-of-practice control and repetitive control for periodic scenario in simulations.

Therefore, the tracking error is fully suppressed. Note that the patient flow and airway pressure are significantly different from the case without patient effort, see Section 4.3.2.

5.3.2 Simulations of the periodic scenario with a deep breath

This section gives the simulation results of the periodic scenario with a deep breath scenario. Compared to Section 5.3.1, the only difference is that a deep breath occurs every sixth breath. In Figure 5.5, the airway pressure and patient flow during a deep breath, and the error 2-norm for all 25 breaths is given for the state-of-practice controllers and repetitive controller. Due to the deep breath the tracking performance decreases for all control strategies except the hose resistance compensation. Note that the amplitude of the decrease in tracking performance is determined by the amplitude of the deep breath. The disturbance p_{mus} changes the airway pressure p_{aw}. If the airway pressure p_{aw} changes, the patient flow Q_{pat} changes via (2.4). Due to a change in patient flow Q_{pat}, the outlet flow Q_{out} changes via (2.8). The hose resistance compensation uses a measurement of the outlet flow Q_{out} to determine its control input. No delays are present in simulation and the hose resistance estimation is exact. Therefore, the tracking performance of the hose resistance compensation controller does not change in the presence of the disturbance p_{mus}, in theory. For the repetitive controller, the error 2-norm increases for the deep breath and the breath thereafter. This is explained as follows. Because the L-filter is based on an exact model of the true system, the error 2-norm converges in one breath. Therewith, the repetitive controller learns the error caused by the deep breath in one breath. However, during the breath after the deep breath, the disturbance p_{mus} is of normal size. Since the repetitive control output is based on the deep breath, a tracking error is introduced. However, since p_{mus} does not change in the next breaths, the error 2-norm converges to zero again. This process occurs during every deep breath , i.e., every sixth breath. Although the tracking performance for the repetitive controller decreases during a deep breath, the repetitive controller has the lowest error 2-norm compared to the state-of-practice controllers.

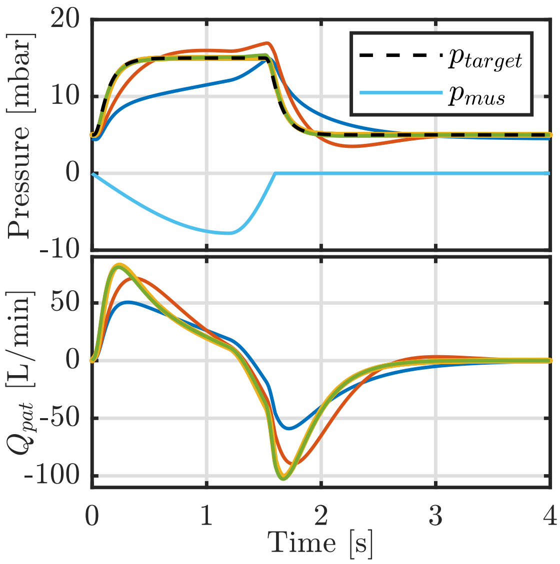

(a) Airway pressure p_{aw} and patient flow Q_{pat} during a deep breath (breath 23).

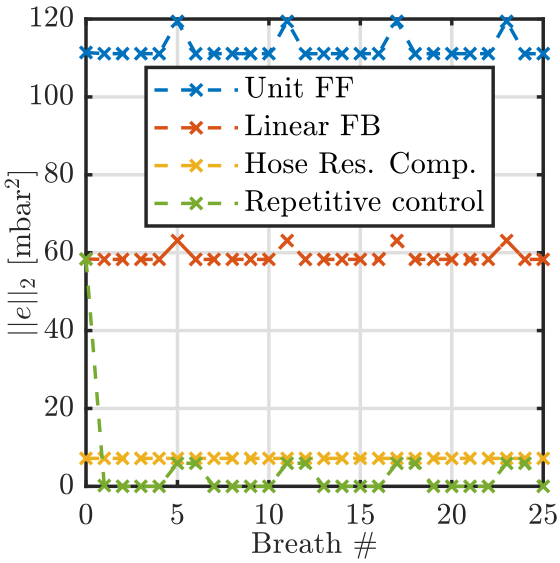

(b) Error 2-norm of 25 breaths.

Figure 5.5. State-of-practice control and repetitive control for periodic scenario with a deep breath in simulations.

5.3.3 Simulations of the aperiodic scenario

This section gives the simulation results of the aperiodic scenario. In Figure 5.6, the airway pressure and patient flow of the last breath, and the error 2-norm for all 25 breaths is given for the state-of-practice controllers and repetitive controller. It is observed that the hose resistance compensation has the best tracking performance compared to the other state-of-practice controllers and repetitive controller. Also, the tracking performance of the hose resistance compensation controller is not affected by the disturbance p_{mus}, see Section 5.3.2. The error 2-norm of the repetitive controller converges to a bound of ± 10 mbar^2 around ≈ 20 mbar^2. This increase in error 2-norm is expected, since the repetitive controller has a constant buffer length, namely 2000, i.e., the number of samples in p_{target}. However, the disturbance p_{mus} changes randomly in length, between 2000-2500 samples, for each breath. Therefore, the disturbance p_{mus} is aperiodic with the period length N, which is not rejected by the repetitive controller, but even amplified. Hence, the attenuation of the aperiodic disturbance p_{mus} relies only the linear feedback controller C. Since C is tuned for robustness, the aperiodic disturbance p_{mus} affects the tracking performance significantly. Therefore, the error 2-norm does not converge to zero, even though a unitary Q-filter is used. A possible solution to reduce amplification of the aperiodic disturbance p_{mus}, is to use a learning gain α as explained in Section 3.4.1. Therewith, however, the convergence rate of the error 2-norm decreases. No further research is done on the influence of a learning gain on aperiodic patient effort.

5.4 Experiments of spontaneously breathing scenarios

This section presents the experimental results of the spontaneously breathing scenarios. These results are used to compare the state-of-practice controllers and the repetitive controller in experiments. During all experiments the best repetitive controller of Section 4.5.2, i.e,. based on a fit of an average FRF tuned with slightly more robustness, is used. In all experiments, the ASL 5000 breathing simulator (IngMar Medical, Pitsburgh, PA) is used, to emulate the patient with spontaneous breathing activity, see Section 4.1. In

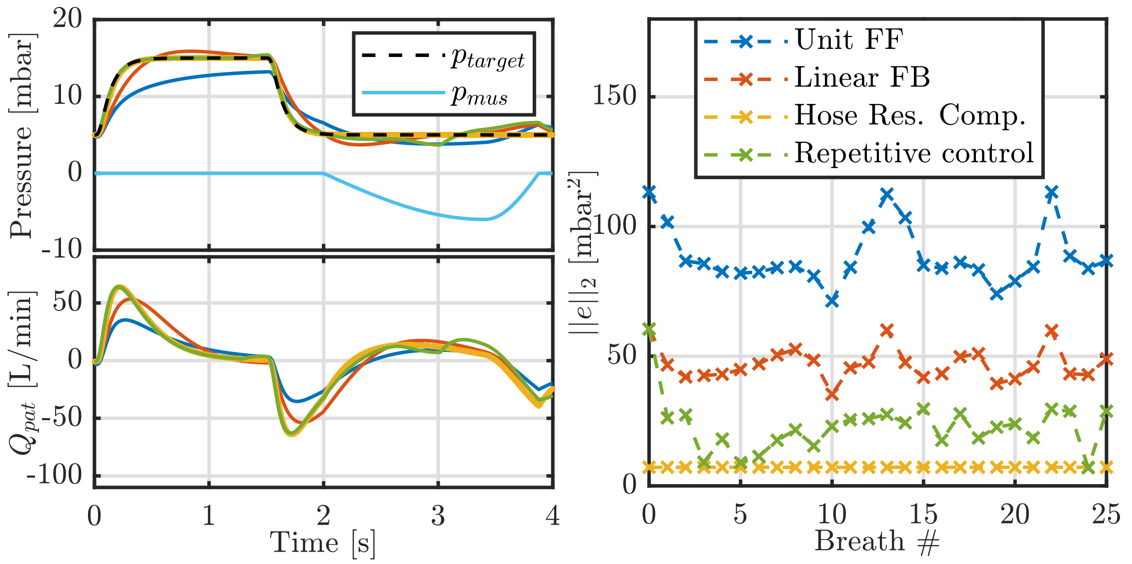

(a) Airway pressure p_{aw} and patient flow Q_{pat} after convergence of the repetitive controller (breath 25).

(b) Error 2-norm of 25 breaths.

Figure 5.6. State-of-practice control and repetitive control for aperiodic scenario in simulations.

Section 5.4.1, the periodic scenario is discussed. Subsequently, the periodic scenario with a deep breath is discussed in Section 5.4.2. Finally, in Section 5.4.3, the aperiodic scenario is discussed.

5.4.1 Experiments of the periodic scenario

Here, the experimental results on the periodic scenario are shown. In Figure 5.7, the airway pressure and patient flow of the last breath, and the error 2-norm for all 25 breaths is given for the state-of-practice controllers and repetitive controller. Using the same methodology as Section 5.3.1, it is observed that the repetitive controller achieves significantly better tracking performance than the state-of-practice controllers. However, blower clipping occurs during expiration for all controllers, except the feedforward controller, indicated by the gray area in Figure 5.7a. This blower clipping is caused by the fact that the blower rpm has a (physical) lower-bound of 1000 RPM. During the blower clipping, the controller desires for a rotational speed of the blower lower than 1000 RPM to decrease the patient flow Q_{pat} fast enough to ensure a good pressure tracking performance. However, the blower is clipped at 1000 RPM. All controllers, except the unit feedforward controller, try to compensate for the error present at the time the blower clips since feedback is used. However, the blower cannot physically turn slower. Therefore, the tracking error cannot be rejected. Hence, a bad airway pressure tracking performance results. Compared to the fully sedated adult scenario of Section 4.5.2, it is observed that the patient flow Q_{pat} for the periodic patient effort scenario is significantly higher. Also, the pressure fall-time is unchanged in the periodic scenario. Thus, the blower needs to decrease the higher patient flow in the same time to ensure good pressure tracking performance in the periodic scenario. This is only achieved if the blower turns slower.

In the repetitive controller, the blower input $p_{control}$ during clipping keeps getting lower with every breath, due to the learning process. This is known as the windup problem [23], which is caused by the fact that the repetitive controller consists of a series of integrators.

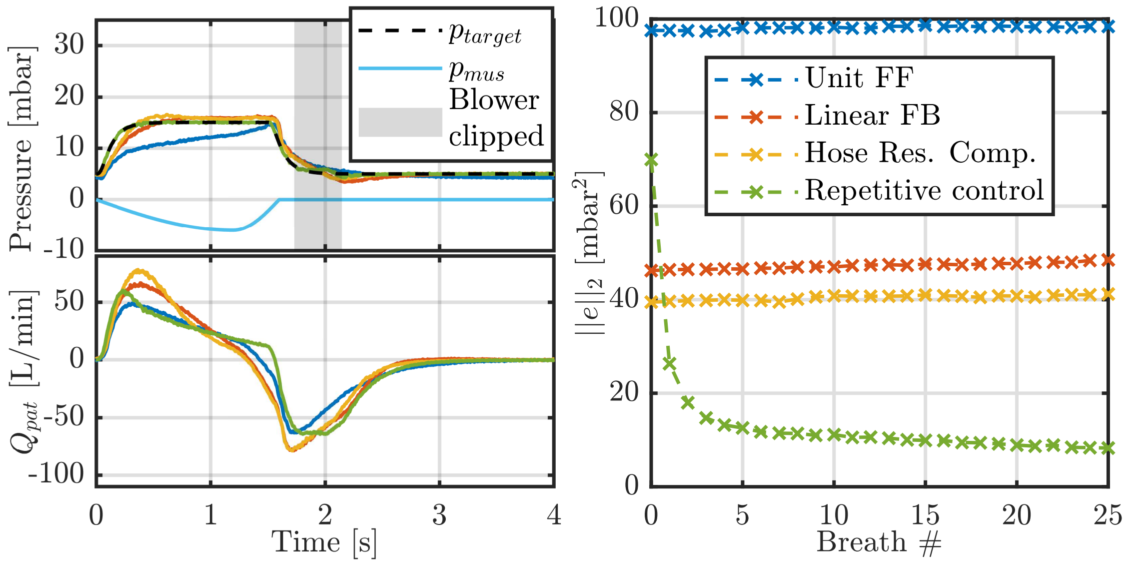

(a) Airway pressure p_{aw} and patient flow Q_{pat} after convergence of the repetitive controller (breath 25).

(b) Error 2-norm of 25 breaths.

Figure 5.7. State-of-practice control and repetitive control for periodic scenario in experiments.

During actuator saturation, the integrators keep integrating, i.e., the repetitive controller keeps learning. However, the actuator is not reacting to the change in input, since it has already reached its boundary value. Therefore, $p_{control}$ keeps growing unbounded, and p_{out} is not following $p_{control}$, see Figure 5.8. It is undesired that $p_{control}$ grows unbounded due to the following. For a moment, consider a scenario where the blower has clipped and, therewith, $p_{control}$ has grown very large. Now assume the patient effort disappears, which means the blower would not clip for a repetitive controller that just starts learning, e.g., see Figure 4.17. However, since the repetitive controller has already learned based on a system with the patient effort, $p_{control}$ is very large. Therefore, the blower still clips and in order to have effect on the pressure tracking, $p_{control}$ first needs to decrease again, which cannot occur instantaneously.

Although blower clipping occurs for every controller, except the feedforward controller, the repetitive controller gives a significantly better tracking performance than the state-of-practice controllers. Therefore, it is advised to use the repetitive controller in the case of periodic patient effort.

5.4.2 Experiments of the periodic scenario with a deep breath

In this section, the experimental results of the periodic scenario with a deep breath are presented. In Figure 5.9, the airway pressure and patient flow during a deep breath, and the error 2-norm for all 25 breaths is given for the state-of-practice controllers and repetitive controller. For this scenario, blower clipping also occurs for every controller, except the feedforward controller. In Figure 5.9a, the gray area indicates where blower clipping occurs. For further details on blower clipping, see Section 5.4.1. In theory, the tracking performance of the hose resistance compensation controller is not changed during a deep breath, as observed in Section 5.3.2. In experiments, however, this is not the case. This is caused by the fact that, in practice, delays are present in the blower and the measurement of p_{aw}. Still, the effect of the deep breath on the hose resistance compensation controller

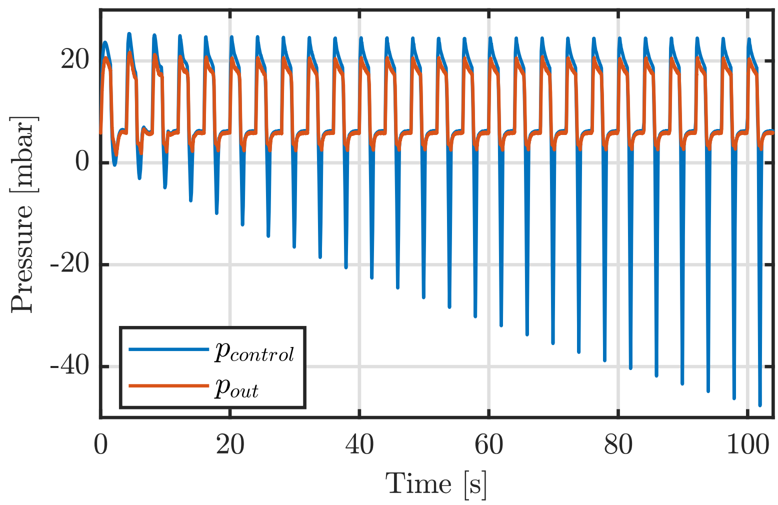

Figure 5.8. Blower in- and output, $p_{control}$ and p_{out}, respectively, over time.

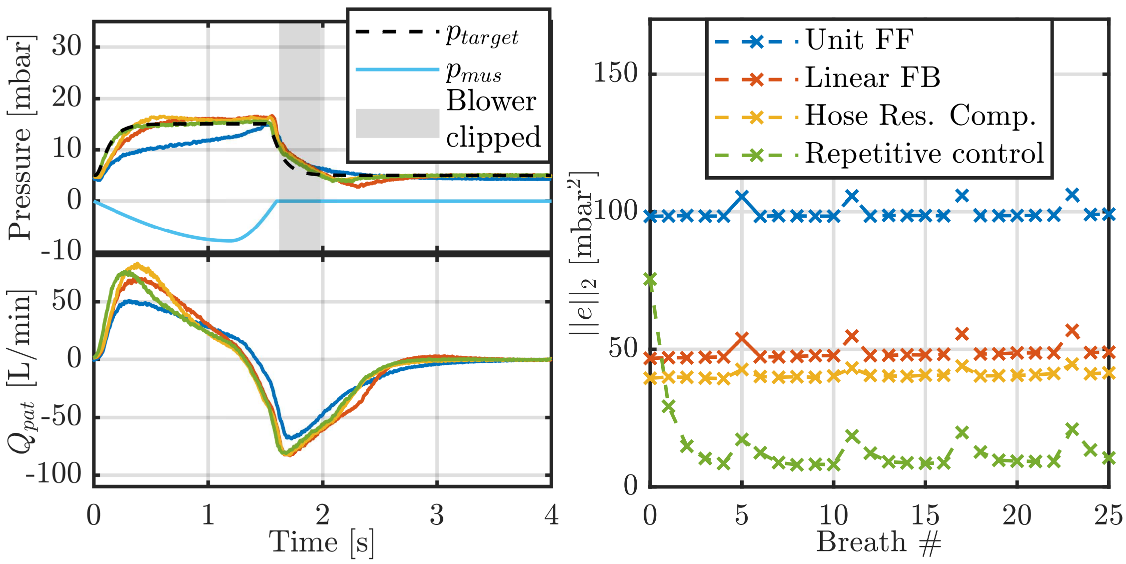

(a) Airway pressure p_{aw} and patient flow Q_{pat} during a deep breath (breath 23).

(b) Error 2-norm of 25 breaths.

Figure 5.9. State-of-practice control and repetitive control for periodic scenario with a deep breath in experiments.

is lower compared to the other controllers. This is seen by the lower increase in error 2-norm during a deep breath for the hose resistance compensation controller.
Although the tracking performance of the hose resistance compensation is affected less by the deep breath and blower clipping occurs for every controller, except the feedforward controller, the repetitive controller has a significantly better tracking performance. Therefore, it is advised to use the repetitive controller in the case of periodic patient effort with a deep breath.

5.4.3 Experiments of the aperiodic scenario

In this section, the experimental results of the aperiodic scenario are presented. In Figure 5.10, the airway pressure and patient flow of the last breath, and the error 2-norm for all 25 breaths is given for the state-of-practice controllers and repetitive controller. It

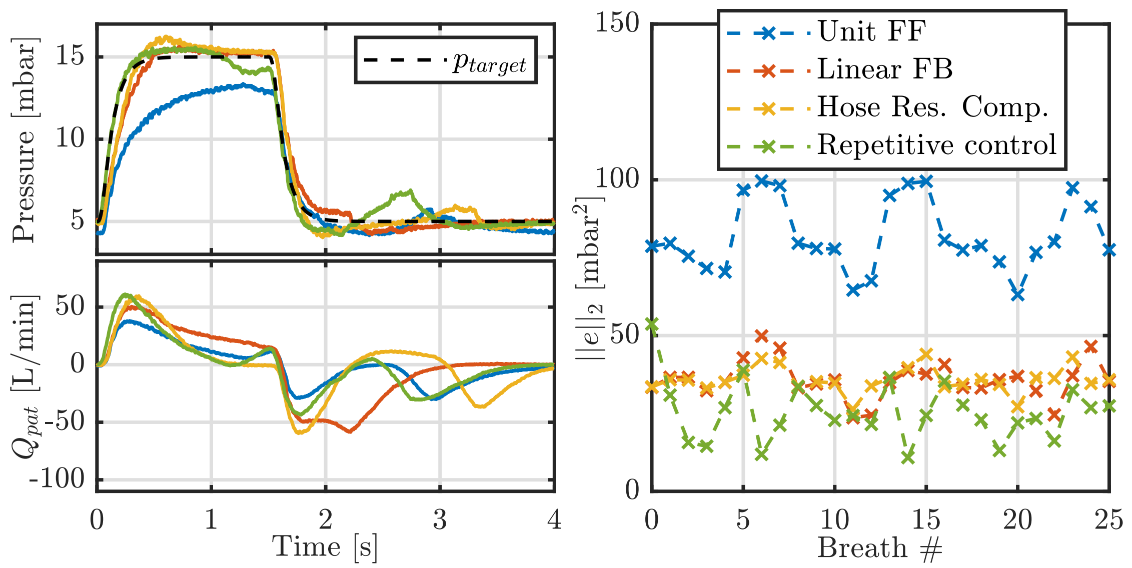

(a) Airway pressure p_{aw} and patient flow Q_{pat} after convergence of the repetitive controller (breath 25).

(b) Error 2-norm of 25 breaths.

Figure 5.10. State-of-practice control and repetitive control for aperiodic scenario in experiments, for typical patient effort profile, see Figure 5.6a.

is observed that the linear feedback, hose resistance compensation, and repetitive controller have similar tracking performance. Similar to Section 5.4.2, it is observed that the tracking performance of the hose resistance compensation controller decreases due to the aperiodic disturbance p_{mus}. Also, the repetitive controller converges to a bound of ± 12.5 mbar^2 around ≈ 22.5 mbar^2 caused by amplification of the significant aperiodic disturbance. Possibly, a learning gain α could decrease the amplification of the aperiodic disturbance. For further details, see Section 5.3.3. In Figure 5.10a, it is observed that, for the depicted breath, the patient flow Q_{pat} has significant overshoot during the pressure plateau phases for the hose resistance compensation controller and repetitive controller. This is caused by the fact that for aperiodic patient effort, the mechanical ventilator and patient are not synchronized due to a varying respiratory rate of the spontaneous breaths. The pressure tracking error at the end of inspiration (1-1.5 s) can be confusing to a physician. In the presence of such a sudden pressure drop, the physician might think that the patient wants to start a spontaneous breath. However, the sudden pressure drop is caused by the fact that the repetitive controller amplifies aperiodic disturbances of previous breaths.

Due to amplification of the aperiodic disturbances by the repetitive controller, the tracking performance compared to the state-of-practice controllers is not significantly improved. The hose resistance compensation is affected less by the aperiodic disturbance. Therefore, it is advised to use the hose resistance compensation in the case of aperiodic patient effort or to further investigate the use of a learning gain in the repetitive controller.

5.5 Summary

In this chapter, repetitive control has been applied to spontaneously breathing patient scenarios. First, in Section 5.1, two challenging scenarios for repetitive control applied to mechanical ventilation have been presented: a target variation due to a change in settings of the mechanical ventilator, and spontaneously breathing patients. Thereafter, the scenarios considered in this chapter have been presented in Section 5.2. These scenarios consist of different spontaneously breathing patient scenarios for untriggered mechanical ventilation. Subsequently, these scenarios have been used to compare the state-of-practice controllers and repetitive control in a simulation and experimental case-study in Section 5.3 and 5.4, respectively. From this case-study, it is concluded that the repetitive controller has a better tracking performance in terms of error 2-norm than the state-of-practice controllers for all scenarios, except the aperiodic scenario. For aperiodic patient effort, the repetitive controller amplifies aperiodic disturbances, which decreases the tracking performance, but also confusing pressure profiles might appear for the physician. Amplification of aperiodic disturbances can be reduced by using a learning-gain, but no further research on this is done in this thesis. In the experiments, it was also observed that blower clipping occurs for all controllers, except the feedforward controller, in both periodic scenarios. Blower clipping decreases the tracking performance significantly. Still, the tracking performance of the repetitive controller is significantly better than the state-of-practice controllers. To conclude, it is adivsed to use the repetitive controller in all scenarios, except the aperiodic scenario. For the aperiodic scenario, it is advised to use the hose resistance compensation controller.

Chapter 6

Conclusions and Recommendations

In this thesis, control of mechanical ventilators has been investigated. The control goal is to ensure good pressure tracking performance of a mechanical ventilator for all possible patient types that are either fully sedated or (partly) spontaneously breathing. The main challenge in achieving this goal is that the same mechanical ventilator must deal with a wide variety of patients, hoses, and filters, i.e., large plant variations. Existing control strategies do not give the desired tracking performance for all plant variations. Breathing has a repetitive nature and, therefore, in this thesis, repetitive control is applied to mechanical ventilation to increase the tracking performance for large plant variations. In Section 6.1, the conclusions of this thesis are presented. Thereafter, recommendations for future research are given in Section 6.2.

6.1 Conclusions

In this section, the conclusions of this thesis are presented. In Section 1.3, the research goal for this thesis, including sub-questions, are given. Next, the sub-questions are discussed individually, thereafter, the research goal is discussed.

How to design a repetitive controller that gives a good tracking performance of a mechanical ventilator for fully sedated patient scenarios?

Four repetitive controllers have been designed in Section 4.4. The first two repetitive controllers are based on a first-principle model, either without or with delays taken into account. Taking delays into account, increases the model quality. Therewith, the repetitive controller can be tuned more for performance instead of robustness. The other two repetitive controllers are based on the fit of an average FRF of the system. One repetitive controller is tuned with slightly more robustness for plant variations than the other. A comparison of tracking performance for all repetitive controllers has been made in Section 4.5.1. This comparison has shown that the repetitive controller based on a fit tuned with slightly more robustness for plant variations, gives the best tracking performance for all considered fully sedated patient scenarios.

How does the designed repetitive controller compare to existing control strategies in fully sedated patient scenarios?

A comparison of the repetitive controller with existing control strategies for fully sedated patient scenarios has been made. Simulations have shown that repetitive control can significantly increase tracking performance compared to existing control strategies for fully sedated patient scenarios, see Section 4.3. However, in simulations, an exact model of the system is available, whereas this is not the case for experiments. In experiments, the repetitive controller based on a fit tuned with slightly more robustness for plant variations is used. The tracking performance of this repetitive controller is significantly better than the tracking performance of the existing control strategies for all considered fully sedated patient scenarios, see Section 4.5.2.

How does the designed repetitive controller compare to existing control strategies in the presence of patient effort?

A comparison of the repetitive controller with existing control strategies in the presence of patient effort has been made. Due to the patient effort, an unknown (possibly) aperiodic disturbance is introduced to the system. The influence of the patient-effort on tracking performance has been investigated in simulation and experimental case-study, see Sections 5.3 and 5.4, respectively. For periodic patient effort, the study shows that, even with a deeper spontaneous breath every six breaths, the tracking performance of repetitive control is significantly better compared to the existing control strategies. In experiments, blower clipping occurs for the periodic scenarios with- or without a deep breath, which limits performance. Still, the tracking performance of the repetitive controller is better compared to the existing control strategies. Therefore, it is advised to use the repetitive controller in the case of periodic patient effort with- or without a deep breath. For an aperiodic patient effort the tracking performance of repetitive controller decreases significantly due to amplification of aperiodic disturbances. No significant difference in tracking performance is observed, compared to the existing control strategies. Due to amplification of aperiodic disturbances confusing pressure profiles might appear for the physician. The amplification of aperiodic disturbances can be reduced by the use of a learning gain. This learning gain reduces the amplification of aperiodic disturbances and, therefore, increases the tracking performance and avoiding confusing pressure profiles, see Section 3.4.1. The hose resistance compensation is less affected by the aperiodic disturbances. Therefore, it is advised to use the hose resistance compensation in the case of aperiodic patient effort or to further research the use of a learning gain for the repetitive controller. Recommendations on future research on repetitive controller with a learning gain applied to mechanical ventilation are given in Section 6.2.3.

Is it possible to apply repetitive control to triggered mechanical ventilation while still obtaining a good tracking performance?

Triggered mechanical ventilation is typically used for spontaneously breathing patients. However, this is a challenging scenario for repetitive control, see Section 5.1. This is due to the fact that the target pressure starts or ends when an inspiratory or expiratory trigger occurs, respectively. Therewith, the timing of the target pressure is unknown and possibly varying over breaths. Thus, it cannot be assumed that the target pressure is periodic. Repetitive control only rejects periodic disturbances. In the case of triggered mechanical ventilation it is, therefore, not guaranteed that repetitive control gives a good tracking performance. No further research has been done on triggered mechanical ventilation. However, it is considered to be the main practical challenge for repetitive control. Recommendations for future research on this subject are made in Section 6.2.1.

Using all previous sub-questions, the research goal is reflected upon.

Investigate the potential and limitations of repetitive control applied to mechanical ventilation.

For fully sedated patient scenarios, repetitive control significantly improves the pressure tracking performance of a mechanical ventilator compared to existing control strategies. However, for spontaneously breathing patient scenarios, challenges arise for repetitive control. For untriggered mechanical ventilation with periodic patient effort with- or without a deep breath, repetitive control improves the tracking performance significantly compared to the existing control strategies. Blower clipping can occur, depending on the settings and scenario. Since blower clipping significantly limits performance, further research is recommended, see Section 6.2.1. For aperiodic patient effort, no significant difference in tracking performance for repetitive control compared to the existing control strategies exists due to amplification of aperiodic disturbances by the repetitive controller. The amplification of aperiodic disturbances also leads to confusing pressure profiles for physicians, however, the amplification of aperiodic disturbances can be reduced by using a learning gain, see Section 6.2.3 for recommendations. It is unsure if repetitive control can be applied to triggered mechanical ventilation. Triggering is considered to be the main (practical) challenge for repetitive control. Recommendations for future research on triggered mechanical ventilation are given in Section 6.2.2.

6.2 Recommendations

This section gives recommendations for future research. In Section 6.2.1, recommendations on future research on blower clipping in the context of repetitive control are given. Thereafter, in Section 6.2.2, recommendations on future research in repetitive control applied to triggered mechanical ventilation are given. Finally, in Section 6.2.3, recommendations on future research on the aperiodic disturbances due to aperiodic patient effort are given.

6.2.1 Blower clipping

In the experiments on spontaneously breathing patient scenarios with periodic patient effort, blower clipping occurs for all control strategies, see Section 5.4. The blower clipping is caused by the fact that the blower has a (physical) lower-bound of 1000 RPM. During the blower clipping, the controller desires for a rotational speed of the blower lower than 1000 RPM in order to ensure a good pressure tracking performance. However, the blower is clipped at 1000 RPM. It is expected that the blower also clips at its upper-bound, i.e., actuator limit, during inspiration for:

- patient effort with higher amplitudes;
- fully sedated patient scenarios with a large (unintended) leak in the system.

For both cases the pressure needs to rise while a significant flow is running, either due to the patient effort disturbance or a significant leak in the system. Therefore, the blower needs to have a high RPM, possibly higher than its physical upper-bound, in order to ensure a good tracking performance. A measurement for a repetitive controller applied to a fully sedated patient scenario with a large leak in the system is given in Figure 6.1. It is observed that the outlet flow Q_{out} does not change during blower clipping. This is as expected since the blower is clipped and cannot turn faster to generate a higher outlet flow Q_{out}. Due to clipping, the tracking performance is significantly reduced. Since blower clipping occurs for almost every controller, significantly limits performance, and occurs for fully sedated- and spontaneously breathing patients, further research is recommended on blower clipping.

Repetitive control consists of a series of integrators and, therewith, the windup problem occurs: during actuator saturation, the integrator keeps integrating, i.e., the repetitive

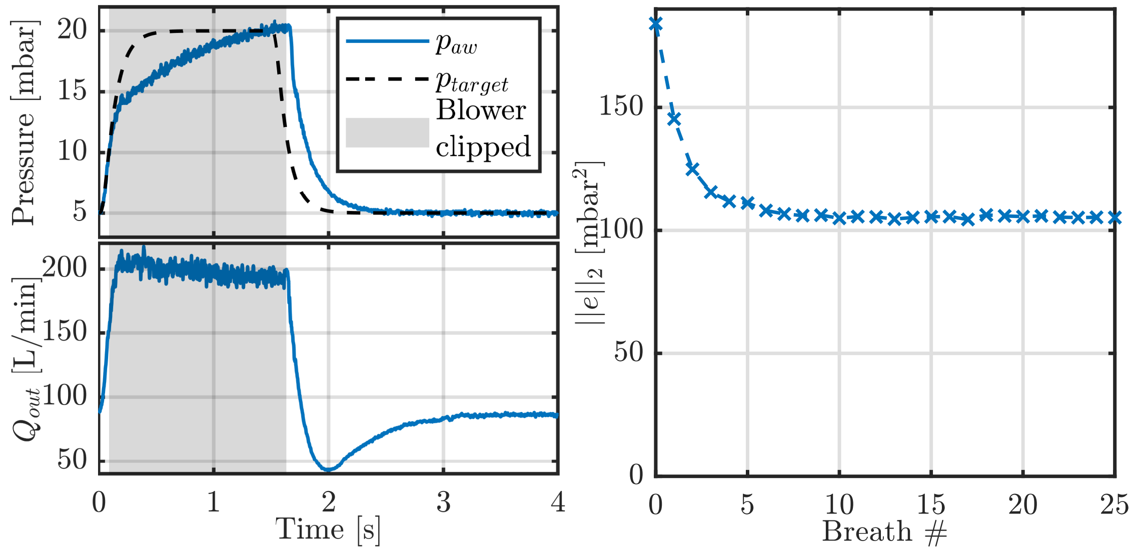

(a) Airway pressure p_{aw} and patient flow Q_{pat} after convergence of the repetitive controller (breath 25).

(b) Error 2-norm of 25 breaths.

Figure 6.1. A measurement of repetitive control applied to mechanical ventilation for a fully sedated patient scenario with a significant leak in the system.

controller keeps learning, i.e., $p_{control}$ keeps getting higher with every breath. However, the actuator is not reacting to the change in input, since it has already reached its boundary value. Therefore, $p_{control}$ keeps growing unbounded, and p_{out} is not following $p_{control}$, see Figure 6.2. It is undesired that $p_{control}$ grows unbounded due to the following. For a moment, consider a scenario where the blower has clipped and, therewith, $p_{control}$ has grown very large. Now assume the large leak disappears, which means the blower would not clip for a repetitive controller that just starts learning, e.g., see Figure 4.17. However, since the repetitive controller has already learned based on a system with the patient effort, $p_{control}$ is very large. Therefore, the blower still clips and in order to have effect on the pressure tracking, $p_{control}$ first needs to decrease again. The decrease of $p_{control}$ cannot occur instantaneously. Therefore, in Figure 6.1a, it is observed that the blower still clips even if the target pressure p_{target} is decreasing already.

In [23] and [31], the windup problem in repetitive control is addressed and anti-windup strategies are proposed. A comparison of different anti-windup strategies is made in [21]. Since blower clipping significantly reduces the tracking performance, it is recommended to further research anti-windup strategies for repetitive control.

6.2.2 Triggered mechanical ventilation

For spontaneously breathing patients, triggered mechanical ventilation is often used in practice. This is considered to be the main (practical) challenge for repetitive control. For further details, see Section 5.1.2 and the conclusion on the last sub-question in Section 6.1. One could assume that the target pressure profile is not changed in terms of rise- and fall-time and constant pressure plateaus. Then, if one assumes that the start and end of the target pressure are determined by a inspiratory or expiratory trigger, respectively, a challenge still remains for repetitive control. This is caused by the fact that the repetitive controller learns with a fixed buffer length and only rejects periodic disturbances. However, the target pressure is aperiodic and varying in length due to triggering at unknown

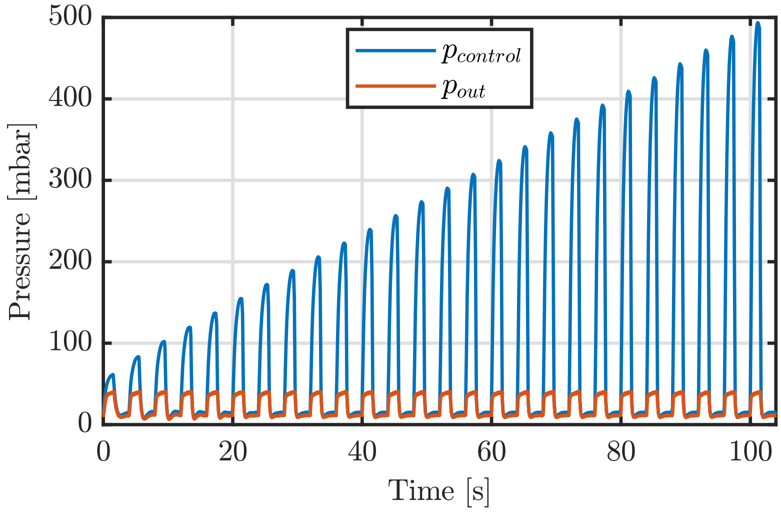

Figure 6.2. Blower in- and output, $p_{control}$ and p_{out}, respectively, over time.

times.

For untriggered mechanical ventilation, the target pressure starts immediately after the end of the previous breath. Since the buffer length of the repetitive controller is equal to the length of a breath length, the repetitive controller learns based on periodic disturbances. For triggered mechanical ventilation, however, the target pressure start and end if a trigger occurs. If only an inspiratory trigger is used and the breath length is fixed, the only unknown is the start of a breath. If an expiratory trigger is also used, the unknowns are the start of a breath and the breath length. Three possible solutions are given next.

- The inspiratory and expiratory trigger occur during constant pressure plateaus, PEEP and IPAP, respectively. Therefore, one could let the repetitive controller only learn a fixed inspiration and expiratory target pressure after an inspiratory or expiratory trigger occurs, respectively. Then, one should hold the last control value of the fixed inspiratory or expiratory target pressure until a trigger occurs.
- A more formal approach is by using a basic task approach [13]. In essence, the same methodology as the first solution is used, i.e., the repetitive controller is only active after a trigger has occurred. However, the repetitive controller uses a library, consisting of previously learned control, or basis, signals, to determine the control values after a trigger has occurred. For instance, the library could consist of basis signals for pressure rise and fall, and constant PEEP- and IPAP pressure for different combinations of rise- and fall-times, and PEEP and IPAP. During operation, the input signal is a concatenation of these individual basis signals.
- Another solution could be to use basis functions [7]. Basis functions parametrize the signal learned by the repetitive controller. The parametrization consists of a linear combination of (user-defined) basis functions ψ_j and parameters θ_j. These parameters are found by computing the least squares optimal values of θ_j such that $\psi_j \theta_j$ matches the learned signal of the repetitive controller as good as possible. For instance, one could use repetitive control with basis functions on a second-order mass-spring-damper system. By choosing the basis functions as the acceleration of the reference, velocity of the reference and the (position) reference, one automatically learn the mass, damping and stiffness of the system. Therewith, tracking performance is obtained for repeating and (slightly) varying tasks.
  The use of basis functions could be interesting to triggered mechanical ventilation, since this method allows for (slightly) varying tasks. The drawback of this method,

however, is that it requires one to design basis functions ψ_j. In mechanical systems, one typically chooses the basis functions as the derivatives of the reference profile. For mechanical ventilation, however, it is unknown what the basis functions should be to obtain a good (pressure) tracking performance. Therefore, further research is required.

6.2.3 Aperiodic disturbances

For repetitive control applied to untriggered mechanical ventilation with aperiodic patient effort, aperiodic disturbances act on the system. This is caused by the fact that the buffer length of the repetitive controller is fixed and corresponds to a fixed respiratory rate of the mechanical ventilator, while the spontaneous breaths have a varying respiratory rate. Therewith, the patient effort is an aperiodic disturbance. Aperiodic disturbances are amplified by the repetitive controller and, therewith, decrease the tracking performance, see Section 3.4.1.

In this thesis, no learning gain has been used, i.e., $\alpha = 1$. However, a learning gain reduces amplification of aperiodic disturbances. Therewith, the error 2-norm upon convergence is decreased. A learning gain also reduces the error 2-norm convergence rate, however. Hence, a trade-off in final error 2-norm and convergence rate exists. Without a learning gain, the error 2-norm convergences in approximately 6 breaths. However, it is acceptable if the error 2-norm convergences slower, e.g., in 15 breaths, which is insignificant to a typical 900 breaths per hour for an adult patient. To obtain both fast convergence and reduce the amplification of aperiodic disturbances, one could use a time-varying learning gain. In this case, the repetitive controller starts without a learning gain to learn on the periodic disturbances caused by the target pressure. If the error 2-norm is converged, the repetitive controller should switch to a lower learning gain, whilst not resetting what was already learned in the case without a learning gain.

Appendix A

Internal delays

In this appendix, the influence of delays on the system is briefly described. The delays are used for controller design in Section 4.4.1. Due to delays in the blower, an input delay of 8 ms is present. In the patient-hose system, it takes time for the pressure propagates through the p_{aw} sensor tube. Therefore, an output delay of 16 ms is present in the patient-hose system. Hence, the open-loop plant contains both in- and output delays. As seen in Section 4.2, the loop is closed around the in- and output delays. Therefore, the in- and output delays are inside the loop. Thus, the closed-loop contains internal delays.
An open-loop with delays is: $L_{delay}(s) = L(s)e^{-N_{del}s}$ with $L(s)$ the open-loop without delays and N_{del} the in- and output delays in seconds. Hence, in- and output delays affect only the phase of a system. An example is given in Figure A.1a. The complimentary sensitivity with delays is: $T_{delay}(s) = \frac{L(s)e^{-N_{del}s}}{1+L(s)e^{-N_{del}s}}$. Hence, internal delays affect the phase and magnitude of a system. An example is given in Figure A.1b.

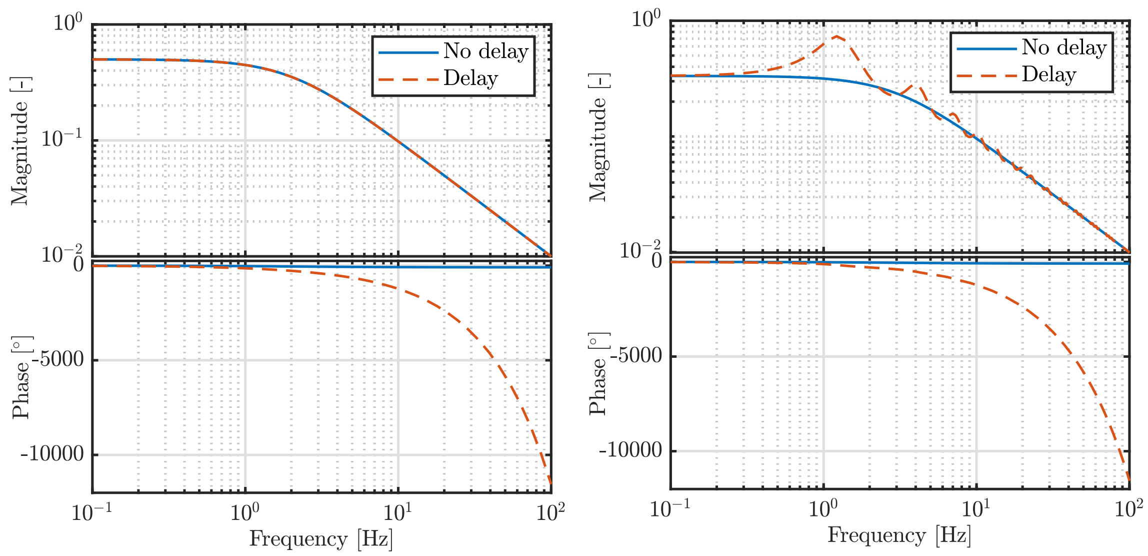

(a) Open-loop: CH.

(b) Complimentary sensitivity: $\frac{CH}{1+CH}$.

Figure A.1. Bode plots for a system with- and without delays in open- and closed-loop, $H = e^{-d_s s}\frac{1}{s+2}$ with d_s 0 or 2 in undelayed and delayed case, respectively, and $C = 1$.

Bibliography

[1] "DEMCON, Macawi." [Online]. Available: https://www.macawi.com/

[2] J. H. Bates, *Lung Mechanics*, 2009.

[3] L. Blanch, "Asynchronies during mechanical ventilation are associated with mortality," *Intensive Care Medicine*, vol. 41, no. 4, pp. 633–641, 2015.

[4] L. Blanken, "Lecture Notes 2017: Advanced Motion Control - Part IX: Repetitive Control," Eindhoven University of Technology.

[5] ——, "Learning and repetitive control for complex systems," Ph.D. dissertation, Eindhoven University of Technology, 2019.

[6] L. Blanken, T. Hazelaar, S. Koekebakker, and T. Oomen, "Multivariable repetitive control design framework applied to flatbed printing with continuous media flow," in *Proceedings of the IEEE Conference on Decision and Control*, Melbourne, Australia, 2017, pp. 4727–4732.

[7] F. Boeren, A. Bareja, T. Kok, and T. Oomen, "Frequency-Domain ILC Approach for Repeating and Varying Tasks: With Application to Semiconductor Bonding Equipment," *IEEE/ASME Transactions on Mechatronics*, vol. 21, no. 6, pp. 2716–2727, 2016.

[8] M. A. Borrello, "Adaptive inverse model control of pressure based ventilation," in *Proceedings of the American Control Conference*, Arlington, VA, USA, 2001, pp. 1286–1291.

[9] B. A. Francis and W. M. Wonham, "The internal model principle for linear multivariable regulators," *Applied Mathematics & Optimization*, vol. 2, no. 2, pp. 170–194, 1975.

[10] E. Gross, M. Tomizuka, and W. Messner, "Cancellation of Discrete Time Unstable Zeros by Feedforward Control," *Journal of Dynamic Systems, Measurement, and Control*, vol. 116, no. 1, p. 33, 2008.

[11] S. Hara and Y. Yamamoto, "Stability of repetitive control systems," in *Proceedings of the IEEE Conference on Decision and Control*, no. 14, 1985, pp. 326–327.

[12] G. Hillerström and K. Walgama, "Repetitive Control Theory and Applications - A Survey," in *Proceedings of the IFAC World Congress*, San Francisco, CA, USA, 1996, pp. 1446–1451.

[13] D. J. Hoelzle, A. G. Alleyne, and A. J. Wagoner Johnson, "Basis task approach to iterative learning control with applications to micro-robotic deposition," *IEEE Transactions on Control Systems Technology*, vol. 19, no. 5, pp. 1138–1148, 2011.

[14] B. Hunnekens, S. Kamps, and N. van de Wouw, "Variable-Gain Control for Respiratory Systems," *IEEE Transactions on Control Systems Technology*, 2017, 10.1109/TCST.2018.2871002.

[15] T. Inoue, M. Nakano, T. Kubo, S. Matsumoto, and H. Baba, "High Accuracy Control of a Proton Synchrotron Magnet Power Supply," in *Proceedings of the IFAC World Congress*, Kyoto, Japan, 1981, pp. 3137–3142.

[16] B. Lachmann, "Open up the lung and keep the lung open," *Intensive Care Medicine*, vol. 18, no. 6, pp. 319–321, 1992.

[17] H. Li and W. M. Haddad, "Model Predictive Control for a Multi-Compartment Respiratory System," in *Proceedings of the American Control Conference*, Montréal, Canada, 2012, pp. 5574–5579.

[18] R. W. Longman, "On the Theory and Design of Linear Repetitive Control Systems," *European Journal of Control*, vol. 16, no. 5, pp. 447–496, 2010.

[19] T. Oomen, "Lecture notes 2017: Advanced Motion Control - Part VII: Iterative Learning Control: Introduction and Frequency Domain Design Approach," Eindhoven University of Technology.

[20] ——, "Learning in machines," *Mikroniek*, vol. 6, pp. 5–11, 2018.

[21] G. A. Ramos, R. Costa-Castelló, and J. M. Olm, "Anti-windup schemes comparison for digital repetitive control," in *Proceedings of the IEEE International Conference on Emerging Technologies and Factory Automation*, Bilbao, Spain, 2010, pp. 1–7.

[22] J. Reinders, F. Heck, B. Hunnekens, T. Oomen, and N. Van de Wouw, "Online hose calibration for pressure control in mechanical ventilation," *(submitted)*.

[23] D. Sbarbaro, M. Tomizuka, and B. L. de la Barra, "The Windup Problem in Repetitive Control: a Simple Anti-Windup Strategy," in *Proceedings of the IFAC World Congress*, 2006, pp. 307–311.

[24] M. Scheel, A. Berndt, and O. Simanski, "Iterative learning control: An example for mechanical ventilated patients," *IFAC-PapersOnLine*, vol. 28, no. 20, pp. 523–527, 2015.

[25] M. Steinbuch, "Repetitive control for systems with uncertain period-time," *Automatica*, vol. 38, no. 12, pp. 2103–2109, 2002.

[26] M. Steinbuch and R. van de Molengraft, "Iterative Learning Control of Industrial Motion Systems," in *Proceedings of the IFAC World Congress*, vol. 33, no. 26, Toulouse, France, 2017, pp. 899–904.

[27] M. Tomizuka, "Zero Phase Error Tracking Algorithm for Digital Control," *Journal of Dynamic Systems, Measurement, and Control*, vol. 109, no. 1, pp. 65–68, 1987.

[28] M. Tomizuka, T.-C. Tsao, and K.-K. Chew, "Analysis and Synthesis of Discrete-Time Repetitive Controllers," *Journal of Dynamic Systems, Measurement, and Control*, vol. 111, no. 3, pp. 353–358, 1989.

[29] D. Torfs, J. De Schutter, and J. Swevers, "Extended Bandwidth Zero Phase Error Tracking Control of Nonminimal Phase Systems," *Journal of Dynamic Systems, Measurement, and Control*, vol. 114, no. 3, p. 347, 2008.

[30] J. Van Zundert and T. Oomen, "An approach to stable inversion of LPTV systems with application to a position-dependent motion system," in *Proceedings of the American Control Conference*, Seattle, WA, USA, 2017, pp. 4890–4895.

[31] Yeong Soon Ryu and R. Longman, “Use of anti-reset windup in integral control based learning and repetitive control,” in *Proceedings of IEEE International Conference on Systems, Man and Cybernetics*, San Antonio, TX, USA, 1994, pp. 2617–2622.